

## Supporting Information

### **Elemental mapping of half-sandwich azopyridine osmium arene complexes in cancer cells**

Elizabeth M. Bolitho<sup>a,b</sup>, Hannah E. Bridgewater<sup>a</sup>, Russell J. Needham<sup>a</sup>, James P. C. Coverdale<sup>a</sup>, Paul D. Quinn<sup>b</sup>, Carlos Sanchez-Cano<sup>c\*</sup>, Peter J. Sadler<sup>a\*</sup>

[a] *Department of Chemistry, University of Warwick, Coventry, UK, CV4 7AL.*

[b] *Diamond Light Source, OX11 0DE, Oxford, OX11 0DE*

[c] *Center for Cooperative Research in Biomaterials (CIC biomaGUNE), Basque Research and Technology Alliance (BRTA), Paseo de Miramon 182, 20014, San Sebastián, Spain*

\* *Corresponding authors:* [paul.quinn@diamond.ac.uk](mailto:paul.quinn@diamond.ac.uk)

[csanchez@cicbiogamune.es](mailto:csanchez@cicbiogamune.es)

[p.j.sadler@warwick.ac.uk](mailto:p.j.sadler@warwick.ac.uk)

<b>ES1 Materials</b>	<b>S3</b>
Chemical reagents	S3
Biological reagents	S3
Human cell lines	S3
<b>ES2 Instrumentation and methods</b>	<b>S4</b>
Nuclear Magnetic Resonance (NMR) Spectroscopy	S4
Mass Spectrometry (MS)	S4
High Performance Liquid Chromatography (HPLC)	S4
Liquid Chromatography- Mass Spectrometry (LC-MS)	S4
pKa studies	S4
Cyclic Voltametry (CV)	S5
Capacity Factor (K)	S5
Plate-reader	S5
Gluthathione (GSH) binding studies)	S5
Inductively-Coupled Plasma Optimal Emission Spectroscopy (ICP-OES)	S5
Inductively-Coupled Plasma Mass Spectrometry (ICP-MS)	S5
Plunge-freezer	S5
Freeze-dryer	S5
Defrosting cells	S5
Passaging cells	S6
Determination of IC <sub>50</sub> values	S6
ICP-OES of stock solutions of complexes	S6
<b>ES3 Time-dependent XRF of A2780 cells treated with 1-PF<sub>6</sub> or 2-PF<sub>6</sub></b>	<b>S7</b>
Figure S1: Fitting of XRF data	S7
Figures S2-S4: XRF maps of untreated A2780 cells	S8
Figures S5-S8: XRF maps of A2780 cells treated with <b>1-PF<sub>6</sub></b>	S9
Figures S9-S14: XRF maps of A2780 cells treated with <b>2-PF<sub>6</sub></b>	S11
Table S1: Cell areas (μm <sup>2</sup> ) and roundness factors	S15
Tables S2-S3: Elemental colocalization statistics	S16
<b>ES4 pK<sub>a</sub> studies</b>	<b>S17</b>
Figures S15-S16: pKa of <b>3-PF<sub>6</sub></b> and <b>4-PF<sub>6</sub></b>	S17
<b>ES5 Glutathione (GSH) binding studies</b>	<b>S18</b>
Figure S17: HPLC/LC-MS chromatograms of <b>3-PF<sub>6</sub></b> and <b>4-PF<sub>6</sub></b> in presence of GSH	S18
Figure S18: LC-MS data showing species found in HPLC chromatograms for <b>3-PF<sub>6</sub></b> and <b>4-PF<sub>6</sub></b> when incubated with GSH	S19
<b>ES6 Cyclic Voltammetry (CV)</b>	<b>S20</b>
Figure S19: Cyclic voltamograms of complexes <b>3-PF<sub>6</sub></b> and <b>4-PF<sub>6</sub></b>	S20
<b>ES7 Osmium (<sup>189</sup>Os) ICP-MS cell accumulation studies</b>	<b>S21</b>
Table S4: Half-maximal inhibitory concentration (IC <sub>50</sub> ) and 24 h osmium cellular accumulation of <b>1-4</b> in A2780 and MRC-5 cells.	S21
Figure S20: Concentration-dependent accumulation of <b>3-PF<sub>6</sub></b> and <b>4-PF<sub>6</sub></b> in A2780 cells	S21
Figure S21: Temperature-dependent accumulation of <b>3-PF<sub>6</sub></b> and <b>4-PF<sub>6</sub></b> in A2780 cells	S21
<b>ES8 Osmium (<sup>189</sup>Os), bromine (<sup>79</sup>Br) and iodine (<sup>127</sup>I) ICP-MS cell accumulation studies</b>	<b>S22</b>
Table S5: Time-dependent cellular accumulation <b>4-PF<sub>6</sub></b> in A2780 cells	S22
Figure S22: Time-dependent cellular accumulation <b>4-PF<sub>6</sub></b> in MRC-5 cells	S22
<b>ES9 Time-dependent XRF of A2780 cells treated with 4-PF<sub>6</sub></b>	<b>S23</b>
Figure S23: Fitting of XRF data	S23
Figures S24-S27: XRF maps of untreated A2780 cells	S24
Figures S28-S33: XRF maps of A2780 cells treated with <b>4-PF<sub>6</sub></b>	S26
Table S6: Cell areas (μm <sup>2</sup> ) and roundness factors	S29
Table S7: Elemental colocalization statistics	S29
<b>ES10 References</b>	<b>S30</b>

## ES1 Materials

**Chemical reagents.**  $\text{OsCl}_3 \cdot 3\text{H}_2\text{O}$  was purchased from Heraeus. The osmium dimer;  $[\text{Os}(\eta^6\text{-}p\text{-cymene})\text{I}_2]_2$  was prepared following previously reported protocols.<sup>1</sup> 5-bromo-2-hydrazinopyridine, *p*-benzoquinone, ammonium hexafluorophosphate, 70% perchloric acid, L-ascorbic acid (BioXtra, >99%), thiourea and sodium chloride (>99%) were purchased from Sigma Aldrich (UK). Sodium hydroxide and 25% *m/v* tetramethyl ammonium hydroxide (TMAH) in water was purchased from Fisher Scientific, and L-glutathione was purchased from Alfa Aesar. Hexachlorodiammonium osmate in 15% *v/v* hydrochloric acid ( $1000 \pm 10 \mu\text{g} / \text{mL}$ ), potassium bromide in water ( $1000 \pm 5 \mu\text{g} / \text{mL}$ ) and ammonium iodide in water ( $1000 \pm 4 \mu\text{g} / \text{mL}$ ) for ICP trace analysis were purchased from Inorganic Ventures. All other organic solvents and reagents for synthesis and analysis were purchased from commercial suppliers and were used as received.

**Biological reagents.** Dulbecco's cell culture medium (DMEM), penicillin/streptomycin, phosphate buffered saline (PBS), heat-inactivated fetal calf serum (FCS), 2 mM L-glutamine, 0.25% trypsin/EDTA and tris-base were purchased from PAA Laboratories and prepared by the technical staff at the School of Life Sciences (University of Warwick). Sulforhodamine B sodium salt Bioreagent was purchased from Sigma Aldrich UK. Trichloroacetic acid (TCA) was purchased from Fisher Scientific.

**Human cell lines.** A2780 (ovarian), A549 (lung) and PC3 (prostate) human carcinoma cell lines and MRC-5 (lung) human fibroblasts were purchased from the ECACC (The European Collection of Cell Cultures). MRC-5 primary lung fibroblasts were used up to a maximum of 5 passages. All cell lines were tested for mycoplasma every 6 months.

## ES2 Instrumentation and methods

**NMR Spectroscopy.**  $^1\text{H}$  NMR spectra were acquired in 5 mm NMR tubes at 25 °C on a Bruker DPX-400 spectrometer. Data processing was carried out using TOPSPIN version 3.2 (Bruker U.K. Ltd).  $^1\text{H}$  NMR chemical shifts were internally referenced to TMS via their residual solvent peaks: acetonitrile ( $\delta = 1.94$  ppm), acetone ( $\delta = 2.05$  ppm), methanol ( $\delta = 3.31$  ppm), water ( $\delta = 4.79$  ppm), chloroform ( $\delta = 7.26$  ppm), DMSO ( $\delta = 2.50$  ppm). Spectra were recorded using standard pulse sequences.

**Mass Spectrometry.** Electrospray mass spectra were obtained using an Agilent 6130B single Quad (ESI) mass spectrometer. Samples of ligands and complexes were typically prepared in methanol or acetonitrile and run in positive ion mode; 50-400 m/z or 500-1000 m/z.

**HPLC.** HPLC analysis of general samples were carried out on an Agilent Technologies 1200 series HPLC instrument with a VWD and 100  $\mu\text{L}$  loop, and an Agilent ZORBAX Eclipse Plus C18 250  $\times$  4.6 mm column with a pore size of 5  $\mu\text{m}$  was used. The mobile phase consisted of; (A) HPLC grade  $\text{H}_2\text{O}$  + 0.1 % TFA, and (B) HPLC grade MeCN + 0.1 % TFA. The following solvent gradient was used with a flow rate of 1 mL/min. Samples were typically prepared at 100  $\mu\text{M}$  and filtered through syringe filters (PTFE, 0.45  $\mu\text{m}$ ). Sample volumes of 100-50  $\mu\text{L}$  were injected into the HPLC column and analysed at a detection wavelength of 254 nm (referenced to 360 and 510 nm). The chromatograms were analysed using ChemStation software and any peaks greater than 10 mAU were integrated.

**LC-MS.** A Bruker Amazon X+ MS instrument coupled to an Agilent Technologies 1200 series HPLC instrument was used. The same HPLC column, method and conditions were used as shown as above, except formic acid was used in place of TFA in the mobile phase, and the flow rate was set to 0.8 mL/min. Samples were injected at 20  $\mu\text{L}$  and the mass spectrometer was operated in electrospray positive mode with a scan range of 50-2000 m/z. Data were analysed using Bruker Data Analysis software.

**pK<sub>a</sub> studies.** Complexes were prepared in aqueous solution (100  $\mu\text{M}$ ) and divided into 1 mL aliquots in glass vials. The pH of the aliquots was adjusted individually by the addition of 1-10  $\mu\text{L}$  of KOH or  $\text{HClO}_4$  (0.01, 0.1, 1, 2, 3, 4, 6, 8 or 10 M), and measured over a range of 1.9 - 12.8 using a pH bench top meter and a micro-combination electrode. Changes in the UV-Vis absorption spectra were recorded at different pH values using disposable polystyrene semi-micro 1.6 mL cuvettes, ensuring no further contact with glass after the pH measurements. Change in intensity of absorbance versus pH was fitted to the Henderson-Hasselbalch equation<sup>29</sup> using Origin 8.5, and the pK<sub>a</sub> was calculated.

**Cyclic voltammetry (CV).** Cyclic voltammetry experiments were conducted using a CH Instruments Electrochemical Analyzer (CHI420C) and CH Instruments electrochemistry software. Measurements were performed using acetonitrile solutions of **3-PF<sub>6</sub>** or **4-PF<sub>6</sub>** (1 mg/mL), containing tetrabutylammonium hexafluorophosphate (0.1 M) as supporting electrolyte. Solutions were degassed under  $\text{N}_2$  and scanned between 0.0 V and -2.0 V at 0.1 V/s. A three-electrode system was used: a glassy carbon electrode as the working electrode,  $\text{Ag}/\text{Ag}^+$  in  $\text{AgNO}_3$  (10 mM in MeCN) as the reference electrode, and platinum wire as the counter electrode.

**Capacity factor ( $K_f$ ).** High Pressure Liquid Chromatography (HPLC) analysis was carried out on an Agilent Technologies 1200 HPLC instrument with a VWD, using an Agilent ZORBAX Eclipse Plus column (C18 250 × 4.6 mm; pore size = 5 μm) and a 100 μL loop. The mobile phase used contained: (i) water + 0.1% trifluoroacetic acid (TFA); (ii) acetonitrile + 0.1% TFA, with a solvent flow rate of 1 mL / min. Samples were typically prepared at 100 μM and syringe-filtered (PTFE, 0.45 μm). Sample volumes of 100-50 μM were injected into the HPLC column and analysed at  $\lambda = 254$  nm (referenced to 360 and 510 nm). The chromatograms were analysed using ChemStation software and any peaks greater than 10 mAU were integrated. Resulting chromatograms were generated using Microsoft Excel 2016. Isocratic HPLC analyses of complexes were carried out. The mobile phase consisted of H<sub>2</sub>O:MeCN (1:1, v/v, 0.1% TFA), and the temperature of the column was kept at a constant (298 K). Samples (500 μM) of **1**, **2**, **3-PF<sub>6</sub>** and **4-PF<sub>6</sub>** were prepared in H<sub>2</sub>O:MeCN (1:1, v/v) and were analysed in triplicate in three separate experiments (50 μL injection volume). Capacity factors ( $K_f$ ) were calculated using the following equation, where  $t_R$  is the retention time of the retained complex,  $t_0$  is the retention time of unretained compound (uracil), and  $R_F$  is the retention factor:

$$K_f = \frac{(t_R - t_0)}{t_0}$$

**Glutathione (GSH) binding studies.** Solutions of **3-PF<sub>6</sub>** and **4-PF<sub>6</sub>** (50 μM) were prepared in phosphate buffer solution (25 mM, pH 7.4) and incubated with 1, 10 or 100 mol eq. of reduced glutathione (GSH at 310 K (0 and 24 h), before storage at 253 K until HPLC/LC-MS analysis. Liquid chromatography mass spectrometry measurements were obtained using a Bruker Amazon X+ instrument coupled to a Agilent 1200 series HPLC. Samples (20 μL) were injected and monitored in by ESI-MS (positive mode, 50 – 2000 m/z). The same HPLC column, method and conditions were used as in the capacity factor studies above, except formic acid was used in place of TFA in the mobile phase, and the flow rate was set to 0.8 mL/min. Samples were injected at 20 μL and the mass spectrometer was operated in electrospray positive mode with a scan range of 50-2000 m/z. Data were analysed using Bruker Data Analysis software.

**Plate-reader.** 96-well plates (SRB assay) were analysed for their UV absorbance (492 nm) using an Biorad iMark microplate reader using Thermo Scientific SkanIt software.

**Plunge-freezing.** Silicon nitride (Si<sub>3</sub>N<sub>4</sub>) membranes were plunge-frozen in 30% liquid propane:ethane mixture cooled with liquid nitrogen using an in-house manufactured plunge-freezer at the School of Life Science (University of Warwick).

**Freeze-drying.** Silicon nitride (Si<sub>3</sub>N<sub>4</sub>) membranes were freeze-dried using an Alpha 2-4 LDplus Christ freeze-dryer operating at -85 °C temperature and 0.0024 mbar vacuum.

**Human cell lines.** A2780 (ovarian), A549 (lung) and PC3 (prostate) human carcinoma cell lines and MRC-5 (lung) human fibroblasts were purchased from the ECACC (The European Collection of Cell Cultures). MRC-5 primary lung fibroblasts were used up to a maximum of 5 passages. All cell lines were tested for mycoplasma every 6 months.

**Defrosting cells.** An frozen ampoule of *ca.* 1-2 × 10<sup>6</sup> cells (stored in cryo-vials in liquid nitrogen) were rapidly defrosted (310 K). The cell solution was resuspended in fully prepared DMEM (supplemented with 10% FCS, 1% penicillin/streptomycin and 1% L-glutamine) and centrifuged (1000 rpm, 298 K, 5 min). The supernatant was removed, the cell pellet resuspended in DMEM (3 mL) and transferred to a T25 cell culture flask for incubation (310 K, 5% CO<sub>2</sub>) until a cell confluency of 80-90% was achieved.

**Passaging cells.** Once 80-90% confluence was achieved, the supernatant media was removed, cells were washed with PBS and trypsinised (0.25% trypsin/EDTA, 1-2 mL, 5 min, 37 °C, 5% CO<sub>2</sub>). Once in solution, DMEM was added and the solution pipetted to form a single cell suspension, and cells were moved to a new culture flask.

**Determination of IC<sub>50</sub> values.** Approximately 5000 cells / well (in 150 µL of fully prepared DMEM) were seeded into F-bottom 96-well plates and incubated at 310 K (48 h, 5% CO<sub>2</sub>). Stock solutions of complexes **1-4** were prepared in 5% v/v DMSO: 95% v/v DMEM and diluted to six concentrations (0.01-100 µM) in DMEM. Cells were treated with different concentrations of osmium complex (in triplicate or duplicate) for 24 h (310 K, 5% CO<sub>2</sub>). The supernatant was removed, cells were washed with PBS and allowed to recover in complex-free media for 72 h (310 K, 5% CO<sub>2</sub>). 50% TCA (50 µL) was added to each well (1 h, 277 K). The plates were washed with water (×10) and air-dried. 0.4% sulforhodamine dye (prepared in 1% acetic acid) was added to each well (50 µL, 30 min). Plates were washed with 1% acetic acid (7×) and heat-dried. 1M pH 10.5 tris-base (100-150 µL) was added to each well and left to stand for 1 h. The UV absorbance (492 nm) was measured using SkanIt multiplate analyser. Data were normalised to the untreated controls, and processed in Microsoft Excel and Origin Lab (sigmoidal dose response). Final IC<sub>50</sub> values were calculated after measuring actual concentration of stock solutions via ICP-OES.

**ICP-OES of stock solutions of complexes.** Prior to cell accumulation studies, stock solutions of osmium complexes (prepared in 5% v/v DMSO; 95% v/v DMEM) were analysed on a Perkin Elmer 5300dv ICP-OES instrument (University of Warwick). A calibration of osmium (0-700 ppb) was prepared in 3.6% v/v nitric acid supplemented with thiourea (10 mM) and L-ascorbic acid (100 mg/L) to prevent formation of volatile osmium tetroxide in acidic conditions. The salinity of the calibration was adjusted with sodium chloride (> 99% purity), to match that of the cell culture medium (DMEM). Prior to all cell accumulation studies, the concentrations of osmium stocks were determined.

## ES3 Time-dependent XRF of A2780 cells treated with 1-PF<sub>6</sub> or 2-PF<sub>6</sub>

### Fitting of XRF data

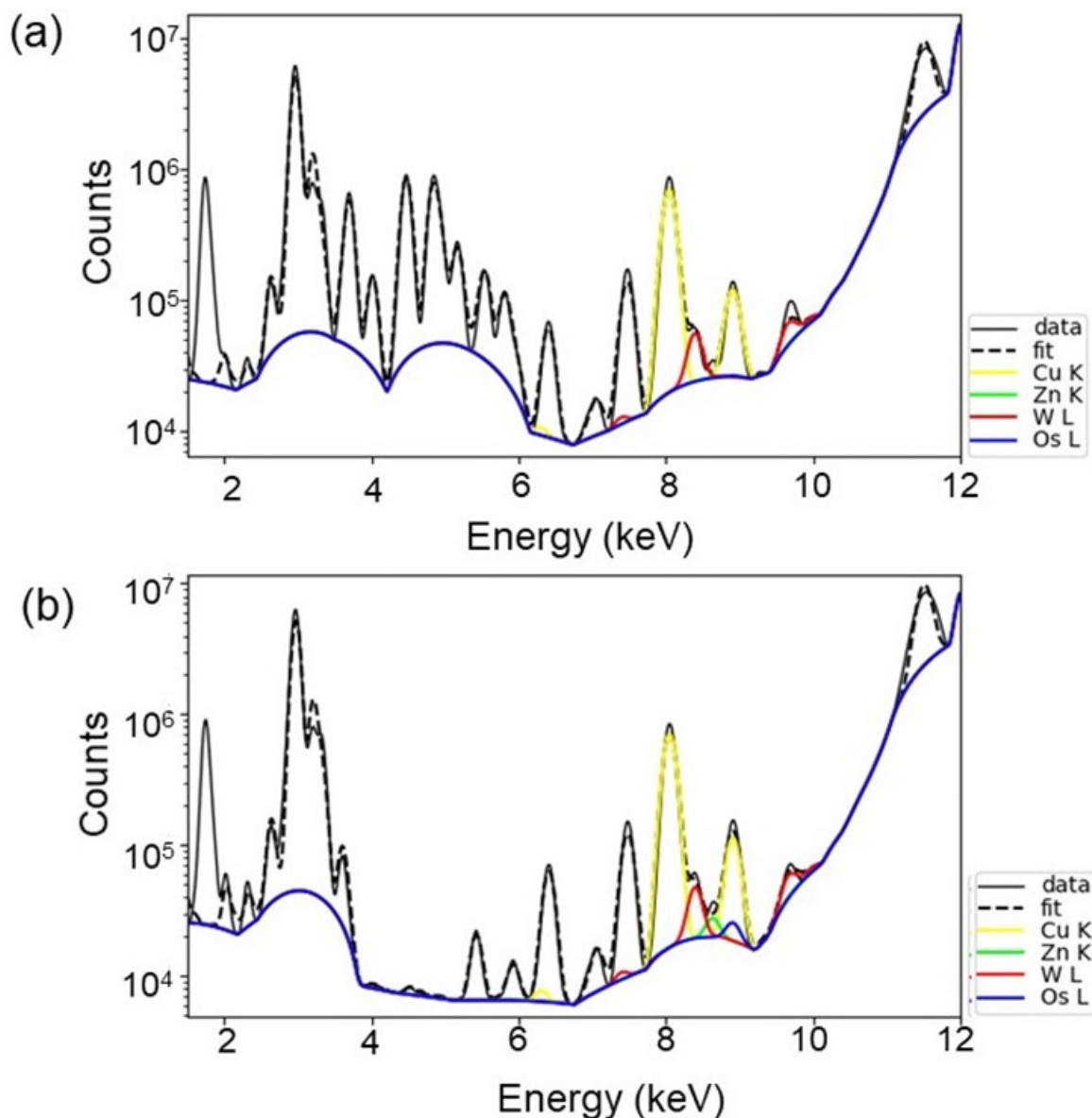


**Figure S1.** Representative XRF spectra for a cryo-fixed and freeze-dried A2780 (human ovarian) cancer cell (0.1 s dwell time, 100 × 100 nm<sup>2</sup>) as obtained by nanofocused synchrotron-XRF. Data were fitted in PyMCA toolkit (ESRF), and selected elements contributing to the emission lines are presented: Cu K (yellow), Zn K (green), W L (red) and Os L (blue). (a) Untreated control (no drug). (b) Cell treated with 7× IC<sub>50</sub> (1 μM) of 2-PF<sub>6</sub> for 8 h (no recovery in drug-free media).

## XRF maps of untreated (control) A2780 cells

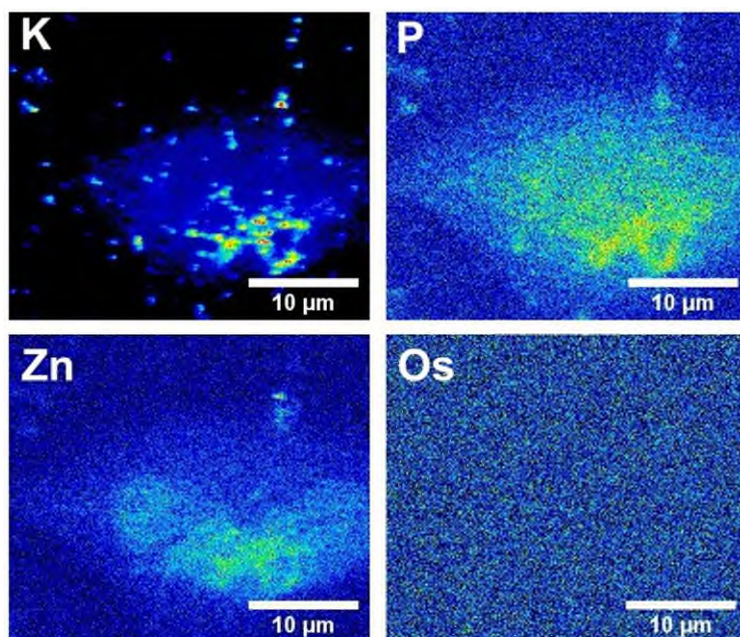


**Figure S2.** Synchrotron-XRF elemental maps of a cryo-fixed and freeze-dried A2780 (human ovarian) cell (**Cell 1, C1**) grown on a  $\text{Si}_3\text{N}_4$  membrane obtained using incident energy 12 keV: K, P, Zn, Os. Maps were collected using 100 nm step size and 0.1 s dwell time. Data were processed in PyMCA toolkit (ESRF),<sup>2</sup> and images were generated in ImageJ for Windows using the 16-colour setting.<sup>3</sup>

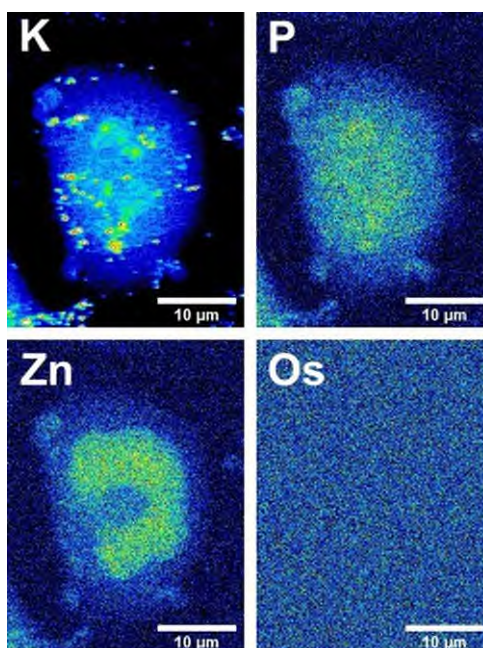


**Figure S3.** Synchrotron-XRF elemental maps of a single, dividing cryo-fixed and freeze-dried A2780 (human ovarian) cancer cell (**Cell 2, C2**) grown on a  $\text{Si}_3\text{N}_4$  membrane obtained using an incident energy of 12 keV: K, P, Zn, Os. Maps were collected using 100 nm step size and 0.1 s dwell time. Data were processed in PyMCA toolkit (ESRF),<sup>2</sup> and images were generated in ImageJ for Windows using the 16-colour setting.<sup>3</sup>



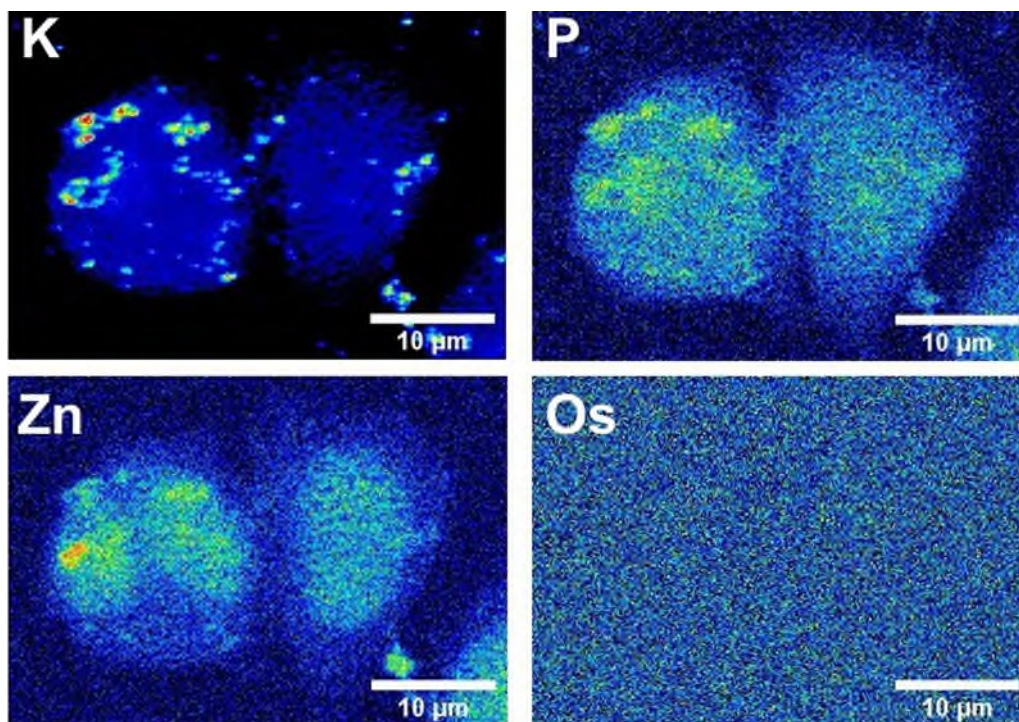


**Figure S4** Synchrotron-XRF elemental maps of a single and a dividing cryo-fixed and freeze-dried A2780 (human ovarian) cancer cells (**Cells 3-4, C3-4**) grown on a  $\text{Si}_3\text{N}_4$  membrane obtained using an incident energy of 12 keV: K, P, Zn, Os. Maps were collected using 100 nm step size and 0.1 s dwell time. Data were processed in PyMCA toolkit (ESRF),<sup>2</sup> and images were generated in ImageJ for Windows using the 16-colour setting.<sup>3</sup>

#### XRF maps of A2780 cells treated with complex 1-PF<sub>6</sub>

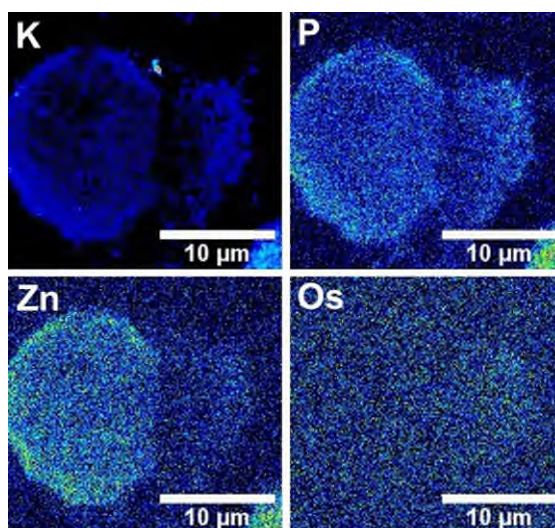


**Figure S5.** Synchrotron-XRF elemental maps of a single cryo-fixed freeze-dried A2780 (human ovarian) cancer cell (**Cell 5, C5**) grown on a  $\text{Si}_3\text{N}_4$  membrane and treated with  $7 \times \text{IC}_{50}$  (12  $\mu\text{M}$ ) **1-PF<sub>6</sub>** for 4 h, obtained using an incident energy of 12 keV: K, P, Zn, Os. Maps were collected using 100 nm step size and 0.1 s dwell time. Data were processed in PyMCA toolkit (ESRF),<sup>2</sup> and images were generated in ImageJ for Windows using the 16-colour setting.<sup>3</sup>



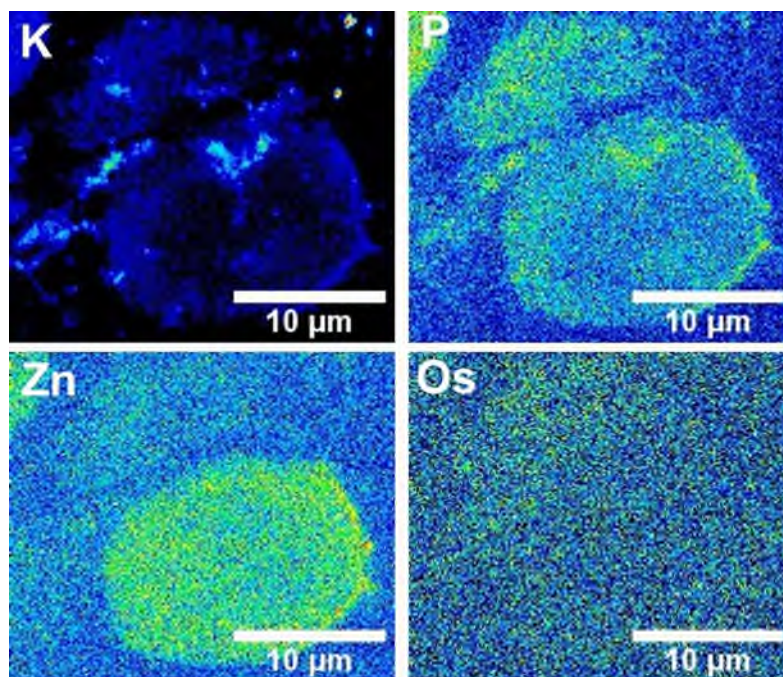


**Figure S6.** Synchrotron-XRF elemental maps of a single cryo-fixed freeze-dried A2780 (human ovarian) cancer cell (**Cell 6, C6**) grown on a  $\text{Si}_3\text{N}_4$  membrane and treated with  $7 \times \text{IC}_{50}$  ( $12 \mu\text{M}$ ) **1-PF<sub>6</sub>** for 4 h, obtained using an incident energy of 12 keV: K, P, Zn, Os. Maps were collected using 100 nm step size and 0.1 s dwell time. Data were processed in PyMCA toolkit (ESRF),<sup>2</sup> and images were generated in ImageJ for Windows using the 16-colour setting.<sup>3</sup>

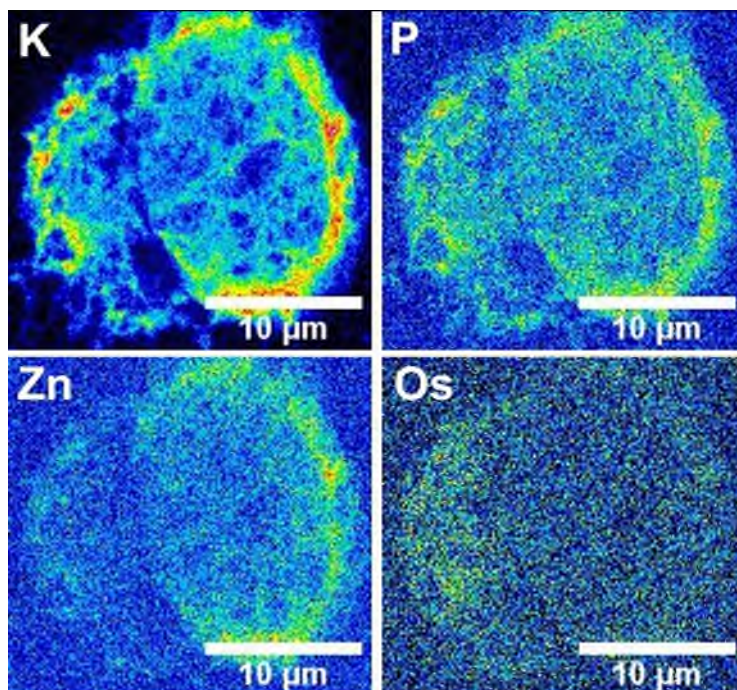


**Figure S7.** Synchrotron-XRF elemental maps of a single cryo-fixed and freeze-dried A2780 (human ovarian) cancer cell (**Cell 7, C7**) grown on a  $\text{Si}_3\text{N}_4$  membrane and treated with  $7 \times \text{IC}_{50}$  ( $12 \mu\text{M}$ ) **1-PF<sub>6</sub>** for 8 h, obtained using an incident energy of 12 keV: K, P, Zn, Os. Maps were collected using 100 nm step size and 0.1 s dwell time. Data were processed in PyMCA toolkit (ESRF),<sup>2</sup> and images were generated in ImageJ for Windows using the 16-colour setting.<sup>3</sup>

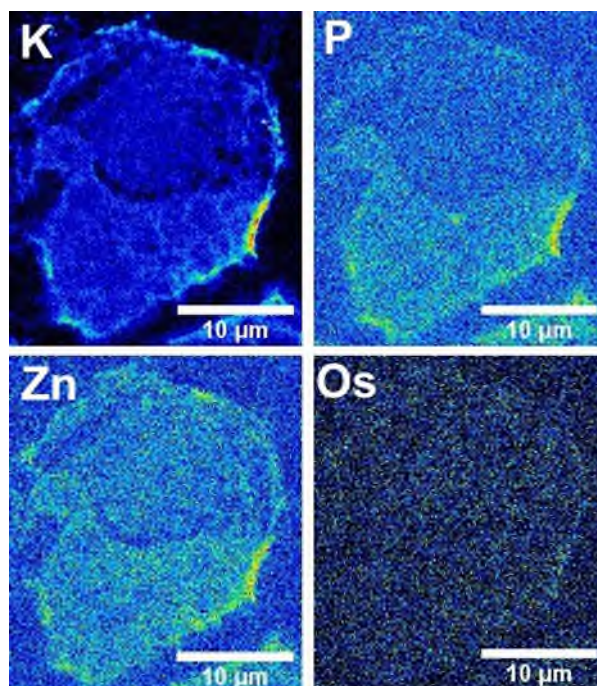


**Figure S8.** Synchrotron-XRF elemental maps of a single cryo-fixed and freeze-dried A2780 (human ovarian) cancer cell (**Cell 8, C8**) grown on a  $\text{Si}_3\text{N}_4$  membrane and treated with with  $7\times \text{IC}_{50}$  ( $12\ \mu\text{M}$ ) **1-PF<sub>6</sub>** for 8 h, obtained using an incident energy of 12 keV: K, P, Zn, Os. Maps were collected using 100 nm step size and 0.1 s dwell time. Data were processed in PyMCA toolkit (ESRF),<sup>2</sup> and images were generated in ImageJ for Windows using the 16-colour setting.<sup>3</sup>

#### XRF maps of A2780 cells treated with 2-PF<sub>6</sub>

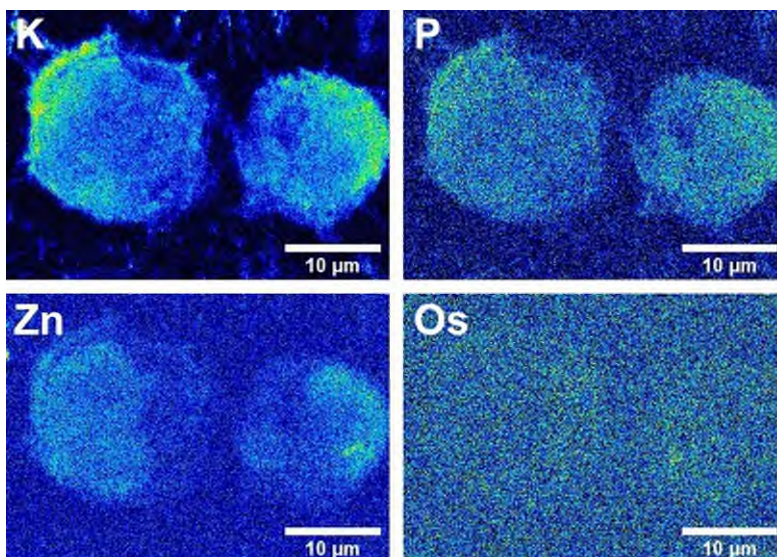


**Figure S9.** Synchrotron-XRF elemental maps of two cryo-fixed and freeze-dried A2780 (human ovarian) cancer cell (**Cells 9-10, C9-10**) grown on a  $\text{Si}_3\text{N}_4$  membrane and treated with  $7\times \text{IC}_{50}$  ( $12\ \mu\text{M}$ ) **2-PF<sub>6</sub>** for 4 h, obtained using an incident energy of 12 keV: K, P, Zn, Os. Maps were collected using 100 nm step size and 0.1 s dwell time. Data were processed in PyMCA toolkit (ESRF),<sup>2</sup> and images were generated in ImageJ for Windows using the 16-colour setting.<sup>3</sup>



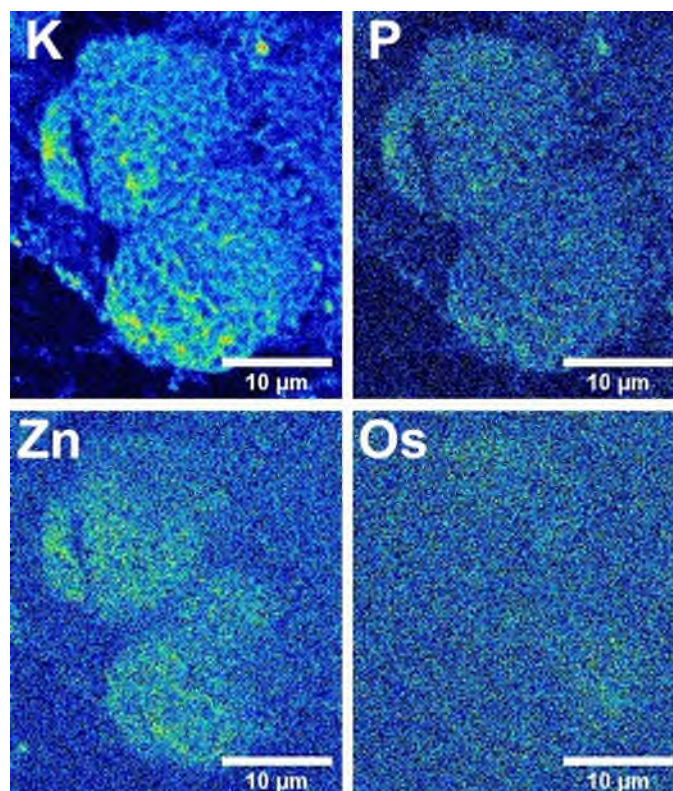


**Figure S10.** Synchrotron-XRF elemental maps of two cryo-fixed and freeze-dried A2780 (human ovarian) cancer cells (**Cells 11-12, C11-12**) grown on a  $\text{Si}_3\text{N}_4$  membrane and treated  $7\times \text{IC}_{50}$  ( $12 \mu\text{M}$ ) **2-PF<sub>6</sub>** for 4 h, obtained using an incident energy of 12 keV: K, P, Zn, Os. Maps were collected using 100 nm step size and 0.1 s dwell time. Data were processed in PyMCA toolkit (ESRF),<sup>2</sup> and images were generated in ImageJ for Windows using the 16-colour setting.<sup>3</sup>

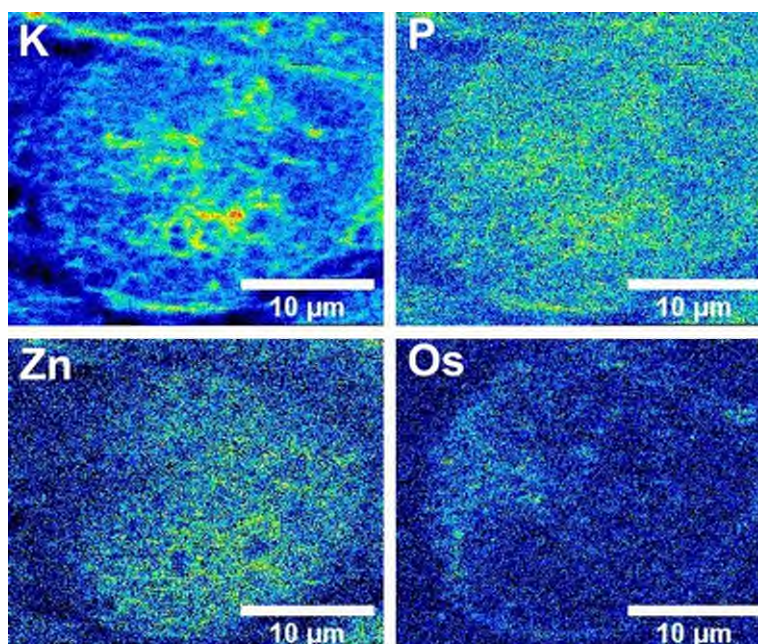


**Figure S11.** Synchrotron-XRF elemental maps of a single cryo-fixed and freeze-dried A2780 (human ovarian) cancer cell (**Cell 13, C13**) grown on a  $\text{Si}_3\text{N}_4$  membrane and treated  $7\times \text{IC}_{50}$  ( $12 \mu\text{M}$ ) **2-PF<sub>6</sub>** for 8 h, obtained using an incident energy of 12 keV: K, P, Zn, Os. Maps were collected using 100 nm step size and 0.1 s dwell time. Data were processed in PyMCA toolkit (ESRF),<sup>2</sup> and images were generated in ImageJ for Windows using the 16-colour setting.<sup>3</sup>



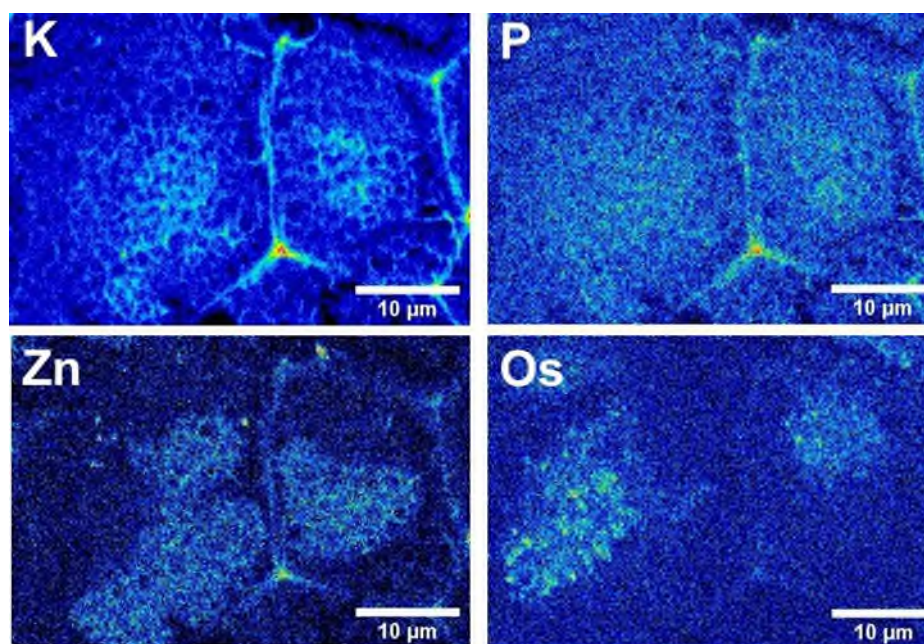


**Figure S12.** Synchrotron-XRF elemental maps of two cryo-fixed and freeze-dried A2780 (human ovarian) cancer cells (**Cells 14-15, C14-15**) grown on a  $\text{Si}_3\text{N}_4$  membrane and treated  $7\times \text{IC}_{50}$  ( $12\ \mu\text{M}$ ) **2-PF<sub>6</sub>** for 8 h, obtained using an incident energy of 12 keV: K, P, Zn, Os. Maps were collected using 100 nm step size and 0.1 s dwell time. Data were processed in PyMCA toolkit (ESRF),<sup>2</sup> and images were generated in ImageJ for Windows using the 16-colour setting.<sup>3</sup>

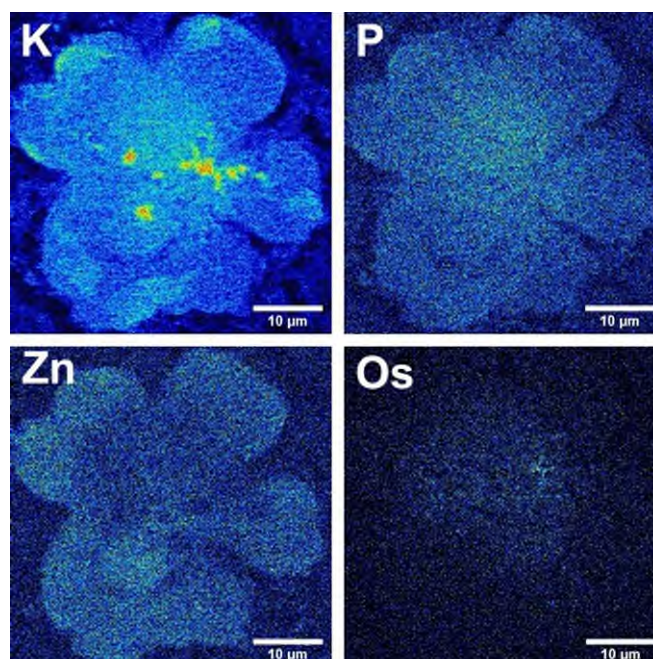


**Figure S13.** Synchrotron-XRF elemental maps of a cryo-fixed and freeze-dried A2780 (human ovarian) cancer cell (**Cell 16, C16**) grown on a  $\text{Si}_3\text{N}_4$  membrane and treated  $7\times \text{IC}_{50}$  ( $12\ \mu\text{M}$ ) **2-PF<sub>6</sub>** for 24 h, obtained using an incident energy of 12 keV: K, P, Zn, Os. Maps were collected using 100 nm step size and 0.1 s dwell time. Data were processed in PyMCA toolkit (ESRF),<sup>2</sup> and images were generated in ImageJ for Windows using the 16-colour setting.<sup>3</sup>

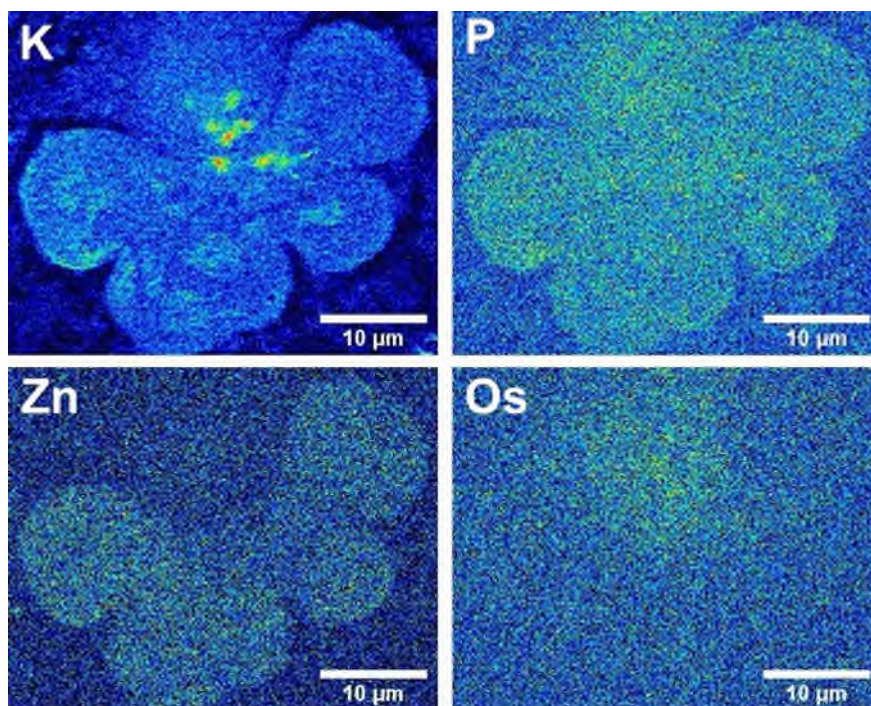


**Figure S14.** Synchrotron-XRF elemental maps of a cryo-fixed and freeze-dried A2780 (human ovarian) cancer cell (**Cell 17, C17**) grown on a  $\text{Si}_3\text{N}_4$  membrane and treated  $7\times \text{IC}_{50}$  ( $12 \mu\text{M}$ ) **2-PF<sub>6</sub>** for 24 h, obtained using an incident energy of 12 keV: K, P, Zn, Os. Maps were collected using 100 nm step size and 0.1 s dwell time. Data were processed in PyMCA toolkit (ESRF),<sup>2</sup> and images were generated in ImageJ for Windows using the 16-colour setting.

## Cell area and roundness factors

**Table S1.** Individual and average cell area ( $\mu\text{m}^2$ ) of cryo-preserved and freeze-dried cells as calculated in triplicate using ImageJ software<sup>3</sup>: (i) incubated in complex-free media for 24 h; (ii) treated with  $7\times \text{IC}_{50}$  ( $12 \mu\text{M}$ ) of **1-PF<sub>6</sub>** for 4 or 8 h; (iii) treated with  $7\times \text{IC}_{50}$  ( $1 \mu\text{M}$ ) of **2-PF<sub>6</sub>** for 4, 8 h or 24 h. No statistically significant differences were observed when using Welch's unpaired t-test, assuming equal variables.

Complex	Cell number	Cell area ( $\mu\text{m}^2$ )	Average cell area ( $\mu\text{m}^2$ )	Roundness Factors	Average Roundness Factor
Controls	1	$326 \pm 4$	$303 \pm 93$	$0.58 \pm 0.04$	$0.77 \pm 0.14$
	2	$439 \pm 3$		$0.96 \pm 0.02$	
	3	$231 \pm 3$		$0.79 \pm 0.03$	
	4	$215 \pm 6$		$0.75 \pm 0.02$	
1-PF <sub>6</sub> (4 h)	9	$312 \pm 17$	$327 \pm 22$	$0.82 \pm 0.03$	$0.79 \pm 0.04$
	10	$342 \pm 20$		$0.76 \pm 0.03$	
1-PF <sub>6</sub> (8 h)	11	$347 \pm 12$	$396 \pm 55$	$0.86 \pm 0.02$	$0.83 \pm 0.04$
	12	$445 \pm 10$		$0.80 \pm 0.01$	
2-PF <sub>6</sub> (4 h)	13	$330 \pm 17$	$403 \pm 275$	$0.91 \pm 0.02$	$0.82 \pm 0.05$
	14	$216 \pm 8$		$0.94 \pm 0.01$	
	15	$242.8 \pm 0.4$		$0.90 \pm 0.04$	
	16	$298 \pm 9$		$0.83 \pm 0.01$	
2-PF <sub>6</sub> (8 h)	17	$388 \pm 4$	$403 \pm 275$	$0.744 \pm 0.001$	$0.84 \pm 0.10$
	18	$598 \pm 18$		$0.82 \pm 0.003$	
	19	$454 \pm 2$		$0.98 \pm 0.003$	
2-PF <sub>6</sub> (24 h)	20	$1485 \pm 12$	$1156 \pm 361$	$0.74 \pm 0.02$	$0.83 \pm 0.10$
	21	$827 \pm 16$		$0.92 \pm 0.01$	

## Co-localisation statistics

**Table S2.** Elemental co-localisation statistics (R-value and Spearman Rank Correlation) between osmium and zinc in cryo-preserved and dehydrated A2780 (human ovarian) cancer cells grown on silicon nitride membranes and treated with  $7 \times IC_{50}$  (12  $\mu$ M) of **1-PF<sub>6</sub>** for 4 or 8 h (no recovery) as determined using Image J software.<sup>3</sup>

Time / h	Cell number	R-value	Mean R-value	Spearman Rank Coefficient	Average Spearman Rank Correlations
4	C5	0.00	0.0 $\pm$ 0.00	-0.002	0.0 $\pm$ 0.003
	C6	0.00		0.002	
8	C7	0.05	0.04 $\pm$ 0.02	0.050	0.03 $\pm$ 0.03
	C8	0.02		0.013	

**Table S3.** Elemental co-localisation statistics (R-value and Spearman Rank Correlation) between osmium and zinc in cryo-preserved and dehydrated A2780 ovarian cancer cells grown on silicon nitride membranes and treated with  $7 \times IC_{50}$  **2-PF<sub>6</sub>** (1  $\mu$ M) for 4, 8 or 24 h (no recovery) as determined using Image J software.<sup>3</sup>

Time / h	Cell	R-value	Mean R-value	Spearman Rank Coefficient	Average Spearman Rank Correlations
4	C9	-0.04	-0.03 $\pm$ 0.03	-0.04	-0.03 $\pm$ 0.03
	C10	-0.04		-0.04	
	C11	-0.05		-0.04	
	C12	-0.05		-0.03	
8	C13	-0.07	-0.06 $\pm$ 0.01	-0.06	-0.06 $\pm$ 0.01
	C14	-0.07		-0.07	
	C15	-0.05		-0.05	
24	C16	-0.04	-0.05 $\pm$ 0.01	-0.03	-0.04 $\pm$ 0.01
	C17	-0.06		-0.05	



## ES4 pK<sub>a</sub> studies

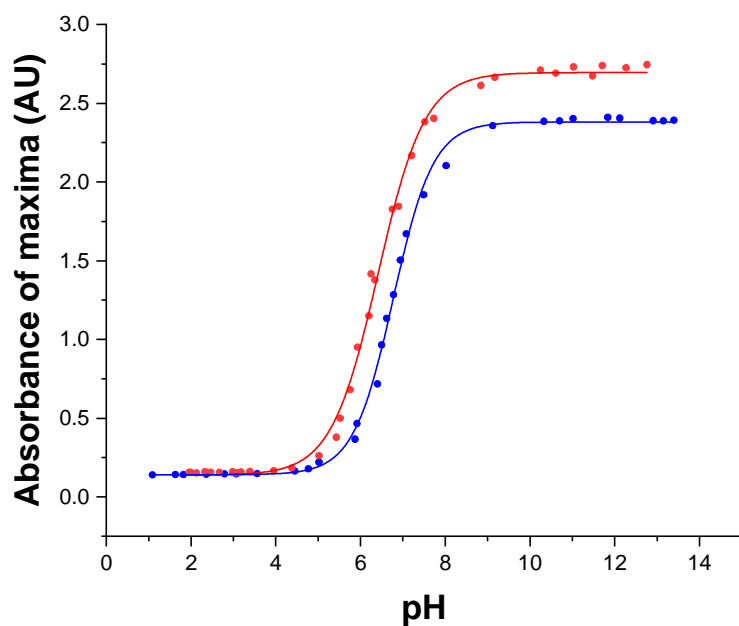


**Figure S15.** Variation of the maximum absorbance of **3-PF<sub>6</sub>** (●, 576 nm) and **4-PF<sub>6</sub>** (●, 588 nm) with pH. The lines represent computational fitting to the Henderson-Hasselbalch equation, with pK<sub>a</sub> values of  $6.78 \pm 0.02$  and  $6.41 \pm 0.02$ , respectively.

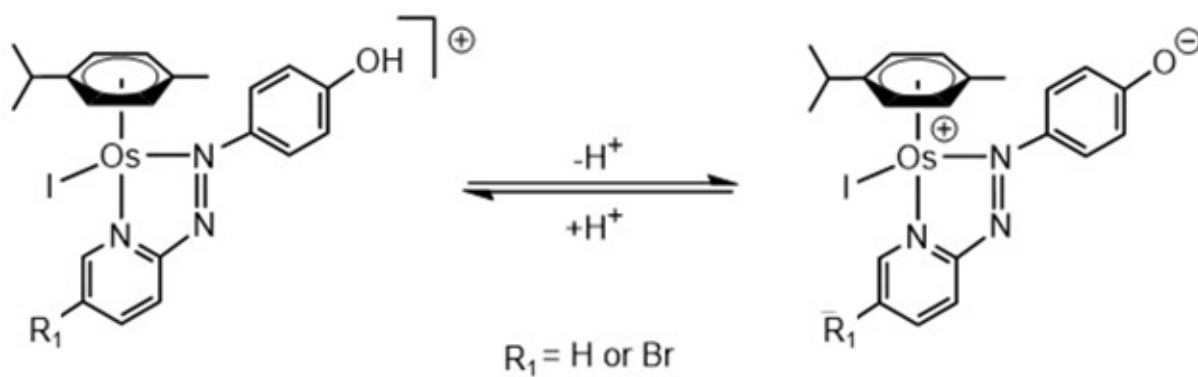


**Figure S16.** Protonation / deprotonation of **3-PF<sub>6</sub>** ( $R_1 = \text{H}$ ) and **4-PF<sub>6</sub>** ( $R_1 = \text{Br}$ ) to their zwitterionic forms.

## ES5 Glutathione (GSH) binding studies

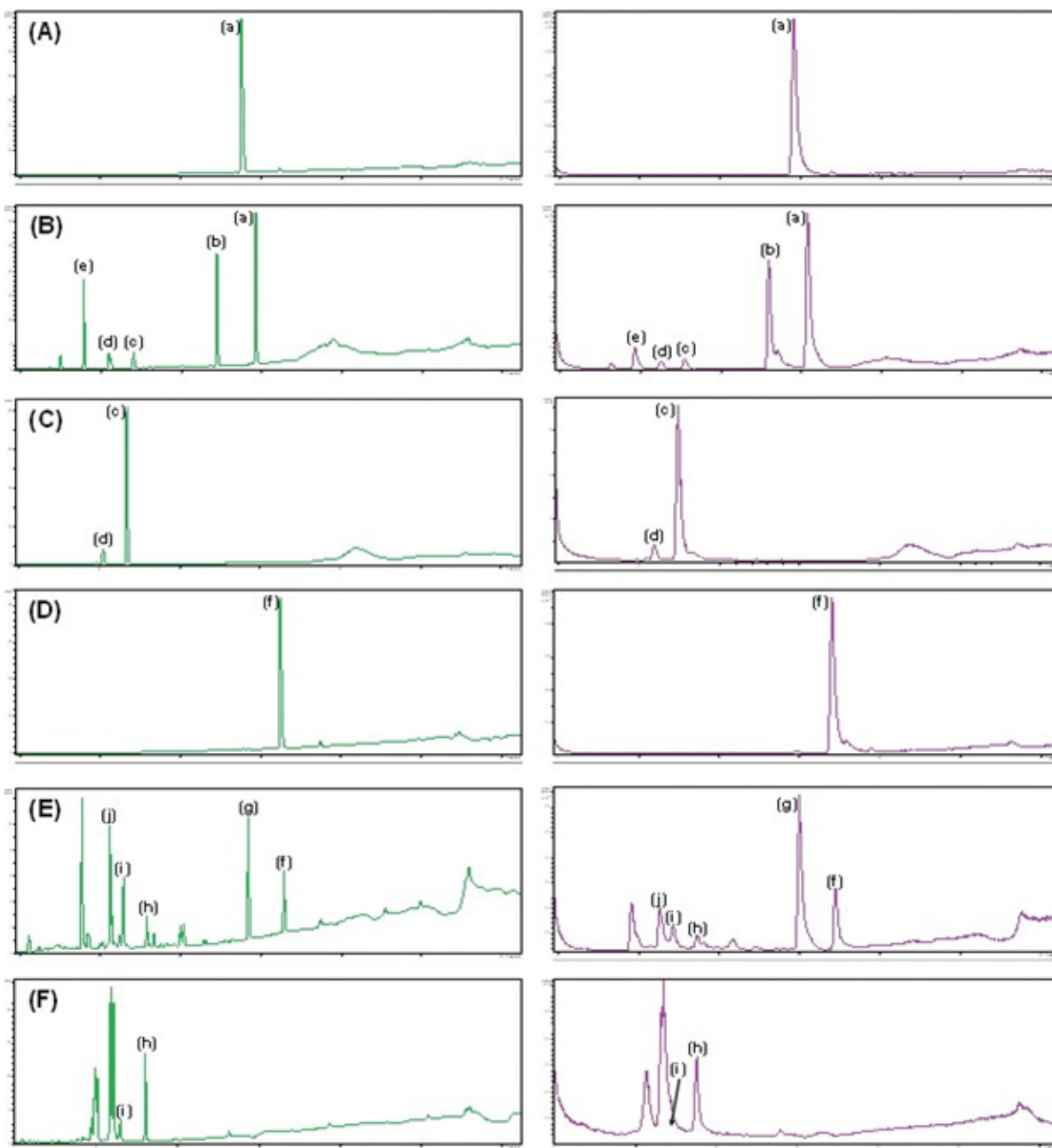


**Figure S17.** HPLC chromatograms (254 nm wavelength of detection, left-hand side), and LC-MS +TIC (total ion count, right-hand side), for 24 h incubation at 37 °C in 25 mM NaCl (pH 7.4) for; (A) 50 μM of **3-PF<sub>6</sub>**, (B) 50 μM of **3-PF<sub>6</sub>** and 10 mol. equiv. GSH, (C) 50 μM of **3-PF<sub>6</sub>** and 100 mol. equiv. GSH, (D) 50 μM of **4-PF<sub>6</sub>**, (E) 50 μM of **4-PF<sub>6</sub>** and 10 mol. equiv. GSH, and (F) 50 μM of **4-PF<sub>6</sub>** and 100 mol. equiv. GSH.

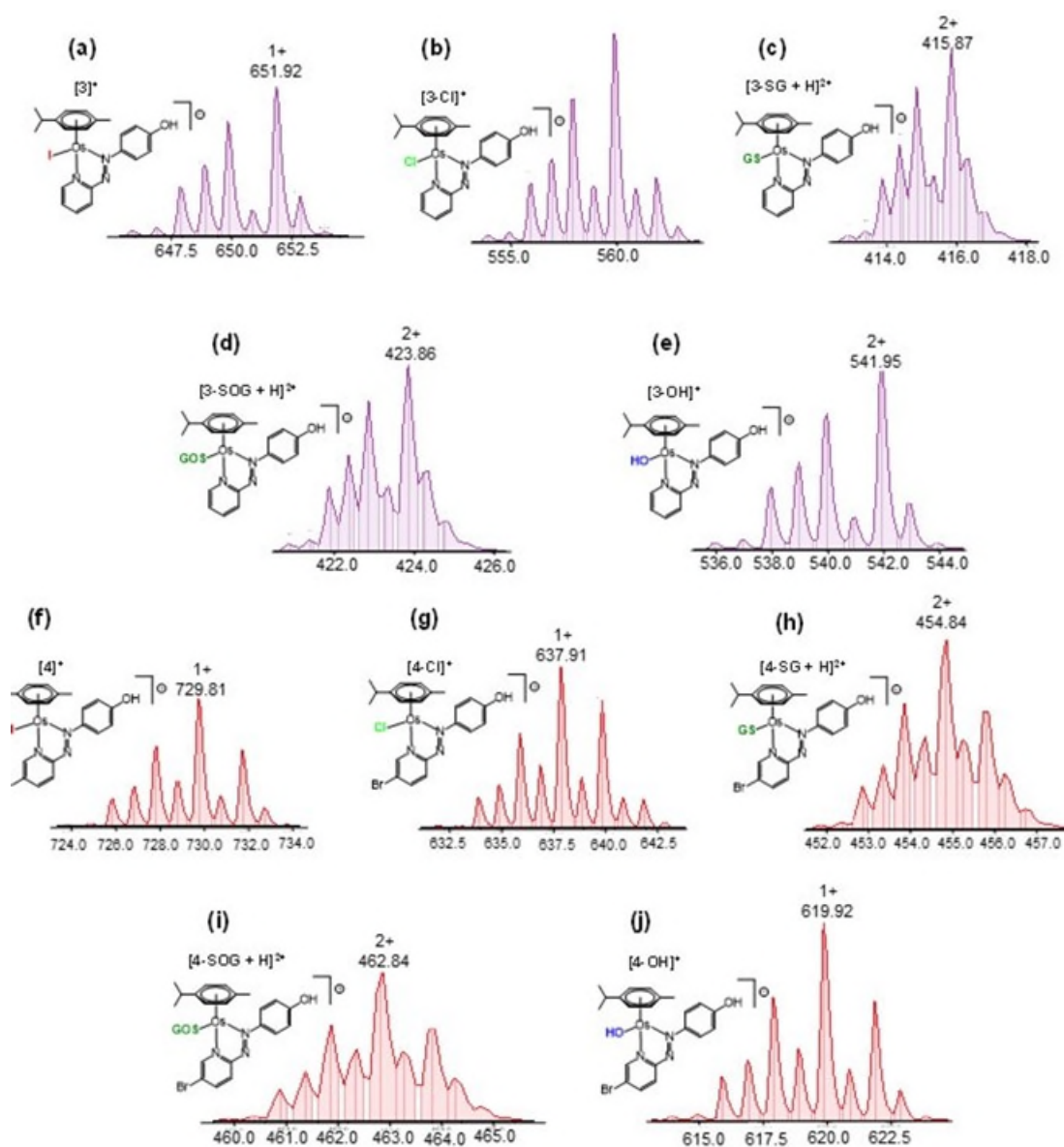


**Figure S18.** LC-MS data showing species found in HPLC chromatograms for **3-PF<sub>6</sub>** and **4-PF<sub>6</sub>** when incubated with GSH. -SG and -SOG refer to thiolato- and sulfenato-adducts of GSH, respectively. All mass spectrometry peaks were observed as positively-charged cations without counter-anions.

## ES6 Cyclic Voltammetry (CV)

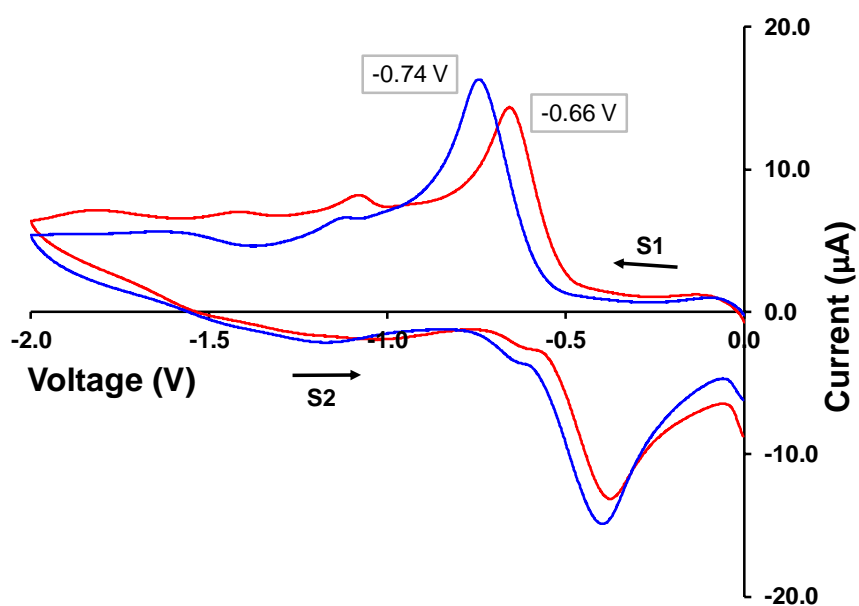


**Figure S19.** Cyclic voltammograms of complexes **3-PF<sub>6</sub>** (-) and **4-PF<sub>6</sub>** (-) in MeCN with 0.1 M Bu<sub>4</sub>NPF<sub>6</sub> as supporting electrolyte, and using Ag/Ag<sup>+</sup> in AgNO<sub>3</sub> (10 mM in MeCN) as the reference electrode. Complexes were scanned from 0.0 to -2.0 V (S1) and back (S2) at 0.1 V/s, and the first azo-bond reduction potentials are -0.66 and -0.74 V, respectively.

## ES7 Osmium ( $^{189}\text{Os}$ ) ICP-MS cell accumulation studies

**Table S4.** Half-maximal inhibitory concentrations ( $\text{IC}_{50}$  /  $\mu\text{M}$ ) and osmium cellular accumulation in A2780 (human ovarian) cancer cells and MRC-5 (healthy lung) fibroblasts.

Complex	A2780 $\text{IC}_{50}$ / $\mu\text{M}$ <sup>[a]</sup>	ng Os / $10^6$ A2780 cells <sup>[b]</sup>	ng Os / $10^6$ MRC-5 cells <sup>[b]</sup>
<b>1-PF<sub>6</sub></b>	$1.8 \pm 0.1$ <sup>[c]</sup>	$7.1 \pm 0.9$	$3.5 \pm 0.4$
<b>2-PF<sub>6</sub></b>	$0.15 \pm 0.01$ <sup>[c]</sup>	$7.7 \pm 0.8$	$2 \pm 0.2$
<b>3-PF<sub>6</sub></b>	$0.51 \pm 0.05$	$5.5 \pm 0.6$	$9.4 \pm 0.7$
<b>4-PF<sub>6</sub></b>	$0.42 \pm 0.03$	$5.9 \pm 0.2$	$11 \pm 2$

<sup>[a]</sup> Anitproliferative activities ( $\text{IC}_{50}$  /  $\mu\text{M}$ ) as determined using the SRB assay 24 h exposure + 72 h recovery in drug-free media. <sup>[b]</sup> Osmium cellular accumulation when treated with the A2780  $\text{IC}_{50}$  concentration for 24 h (no recovery). <sup>[c]</sup> Literature  $\text{IC}_{50}$  values.<sup>4</sup>

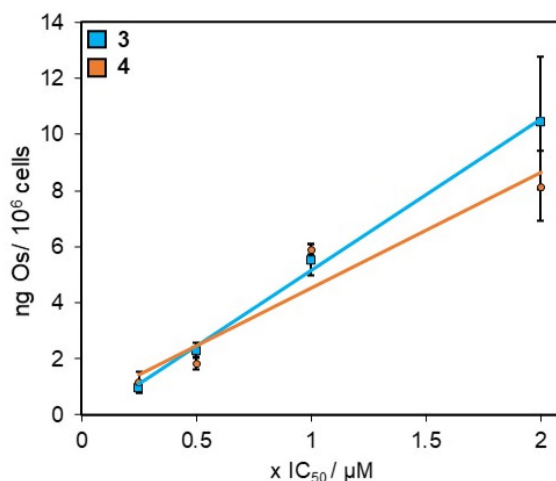


**Figure S20.** Concentration-dependent osmium cellular accumulation of **3-PF<sub>6</sub>** (■) and **4-PF<sub>6</sub>** (■) in A2780 (ovarian) cancer cells treated with equipotent concentrations ( $0-2 \times \text{IC}_{50}$ , where  $\text{IC}_{50}$  is the half-maximal inhibitory concentration after 24 h exposure + 72 h recovery in drug-free media) for 24 h, no recovery.

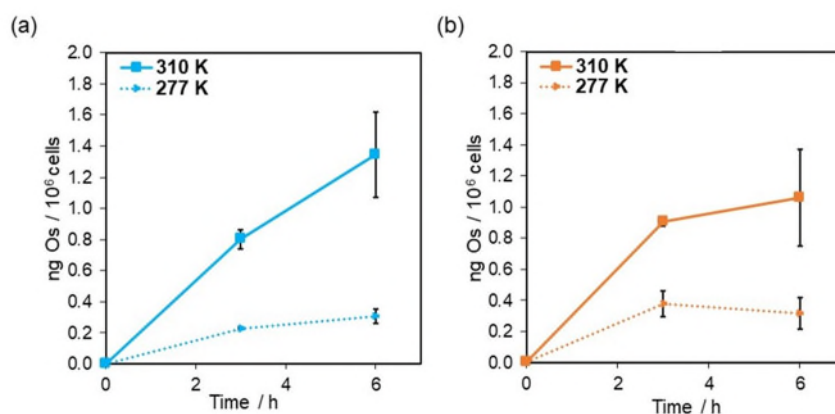


**Figure S21.** Temperature-dependent osmium cellular accumulation from (a) **3-PF<sub>6</sub>** (■) and (b) **4-PF<sub>6</sub>** (■) in A2780 cells treated with equipotent concentrations ( $1 \times \text{IC}_{50}$ , where  $\text{IC}_{50}$  is the half-maximal inhibitory concentration after 24 h exposure + 72 h recovery in drug-free media) for 3 or 6 h at 310 K or 277 K, no recovery time.

## ES8 Osmium ( $^{189}\text{Os}$ ), bromine ( $^{79}\text{Br}$ ) and iodine ( $^{127}\text{I}$ ) ICP-MS cell accumulation studies

**Optimization of TMAH digestion.** A calibration solution containing osmium, bromine and iodine in 1% *m/v* tetramethylammonium hydroxide (TMAH) was prepared in the range 0.1-1000 ppb. ICP-MS calibration curves of  $R^2 = 0.9999$ , 1.0000 and 0.9999 were obtained for osmium ( $^{189}\text{Os}$ ), bromine ( $^{79}\text{Br}$ ) and iodine ( $^{127}\text{I}$ ), respectively. Known solutions of osmium, bromine and iodine analytes were prepared in 1% TMAH in triplicate, in addition to known concentrations of combined Os-Br, Os-I, Br-I and Os-Br-I. Solutions of potassium iodide, potassium bromine and osmium trichloride were prepared directly in 1% *m/v* TMAH or by using the “alkaline digestion” method (*i.e.* digestion in 500  $\mu\text{L}$  25% *m/v* TMAH followed by 1 in 25 dilution). Recoveries >95% for osmium, bromine and iodine were determined for all analysed compounds. The limits of detection for  $^{189}\text{Os}$ ,  $^{179}\text{Br}$  and  $^{127}\text{I}$  were determined to be 0.01 ppb, 1.09 ppb and 0.11 ppb, respectively, when analysed in [He] gas mode.

**Table S5.** Time-dependent osmium and bromine cellular accumulation in A2780 cells treated with of **4-PF<sub>6</sub>** at  $1 \times \text{IC}_{50}$  (0.42  $\mu\text{M}$ ) for 4, 8, 18, 24 h drug exposure and 24 h drug exposures with 24, 48 and 72 h recoveries in drug-free media, and the molar ratio of intracellular Br / Os ratio.

Time / h	ng Os / $10^6$ cells	ng Br / $10^6$ cells	Molar [Br]/[Os]
4	$32 \pm 1$	$9.2 \pm 0.3$	$0.69 \pm 0.04$
8	$25 \pm 3$	$6.7 \pm 0.7$	$0.64 \pm 0.09$
18	$15 \pm 1$	$4.0 \pm 0.2$	$0.64 \pm 0.05$
24	$11 \pm 1$	$2.5 \pm 0.2$	$0.55 \pm 0.07$
48	$4.5 \pm 0.5$	$1.7 \pm 0.3$	$0.92 \pm 0.12$
72	$4.5 \pm 0.2$	$1.6 \pm 0.04$	$1.02 \pm 0.04$
96	$2.3 \pm 0.1$	$1.05 \pm 0.05$	$1.38 \pm 0.05$

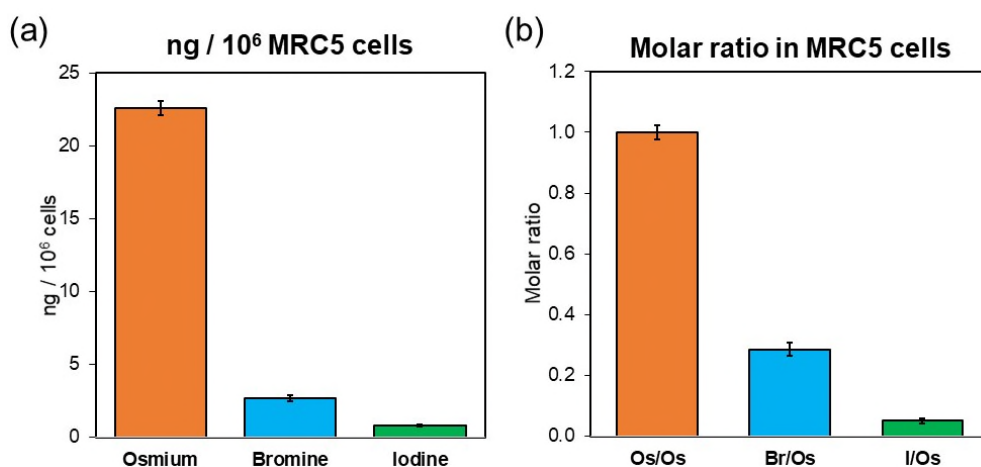


**Figure S22.** (a) Osmium ( $^{189}\text{Os}$ , ■), bromine ( $^{79}\text{Br}$ , ■) and iodine ( $^{127}\text{I}$ , ■) cellular accumulation (ng /  $10^6$  cells) of **4-PF<sub>6</sub>** in MRC-5 healthy lung fibroblasts treated with  $1 \times \text{A2780 IC}_{50}$  (0.42  $\mu\text{M}$ ) of **4-PF<sub>6</sub>** for 24 h (no recovery). (b) Molar ratio of  $^{79}\text{Br}$  and  $^{127}\text{I}$  when normalised to  $^{189}\text{Os}$ , where Os:Br:I ratio is 1:0.29:0.05.

## ES9 Time-dependent XRF of A2780 cells treated with 4-PF<sub>6</sub>

### Fitting of XRF data

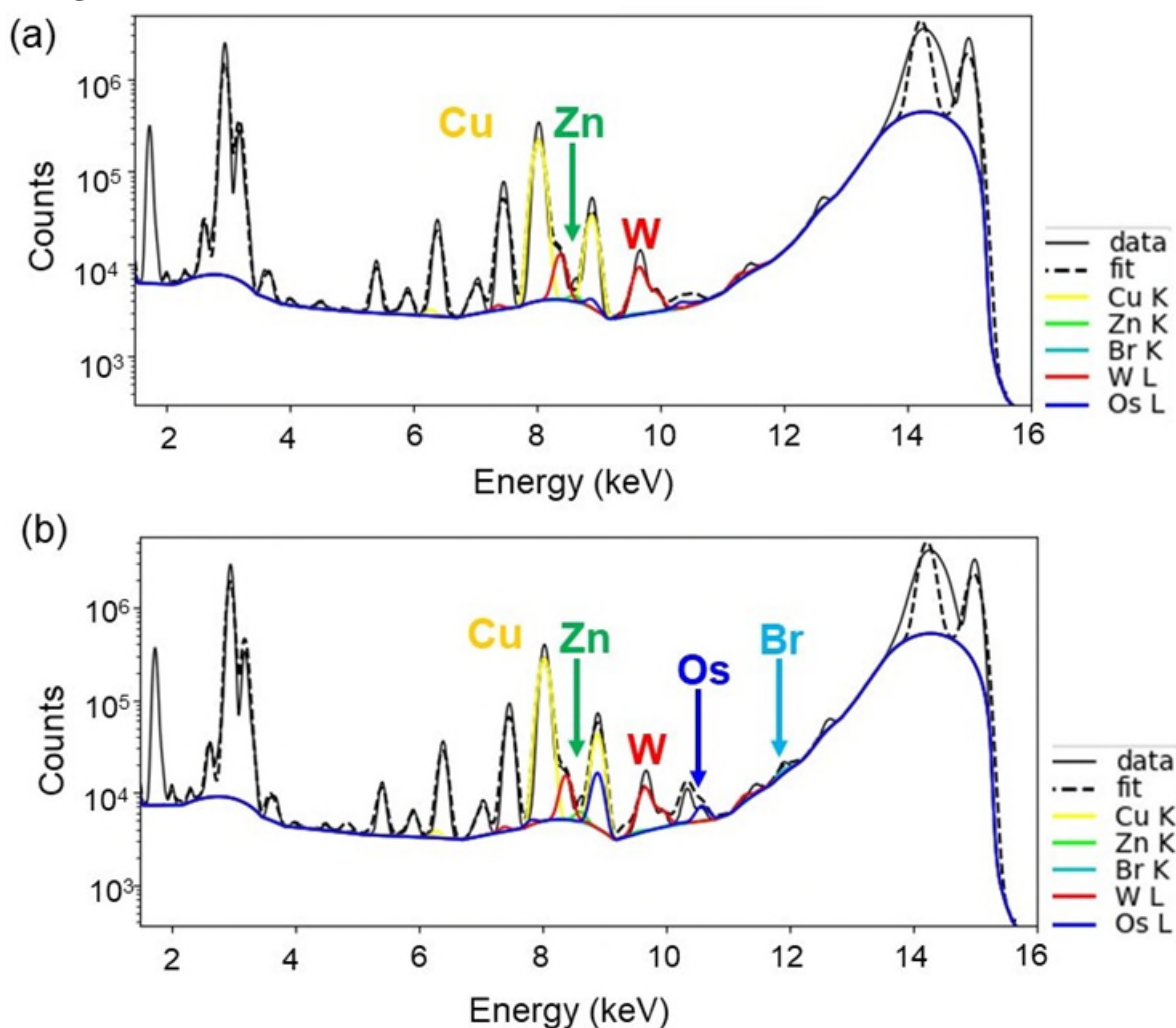


**Figure S23.** Representative XRF spectra for a cryo-fixed and freeze-dried A2780 (human ovarian) cancer cell (0.1 s dwell time,  $100 \times 100 \text{ nm}^2$ ) as obtained by nanofocused synchrotron-XRF. Data were fitted in PyMCA toolkit (ESRF), and selected elements contributing to the emission lines are presented: Cu K (yellow), Zn K (green), W L (red), Os L (blue) and Br K (cyan). (a) Untreated control (no drug). (b) Cell treated with  $7 \times \text{IC}_{50}$  ( $3 \mu\text{M}$ ) of 4-PF<sub>6</sub> for 8 h (no recovery in drug-free media).



### XRF maps of untreated (control) cells

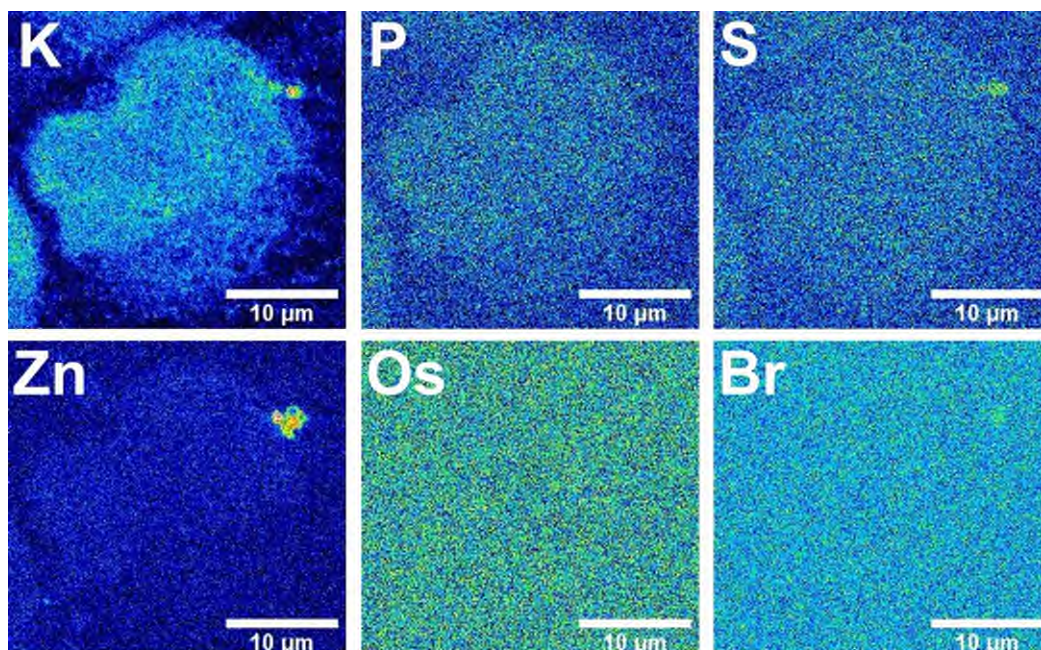


**Figure S24.** Synchrotron-XRF elemental maps of a single cryo-fixed and freeze-dried A2780 (human ovarian) cancer cell (Cell 18, C18) grown on a  $\text{Si}_3\text{N}_4$  membrane obtained using an incident energy of 15 keV: K, P, S, Zn, Os and Br. Maps were collected using 100 nm step size and 0.1 s dwell time. Data were processed in PyMCA toolkit (ESRF),<sup>2</sup> and images were generated in ImageJ for Windows using the 16-colour setting.<sup>3</sup>

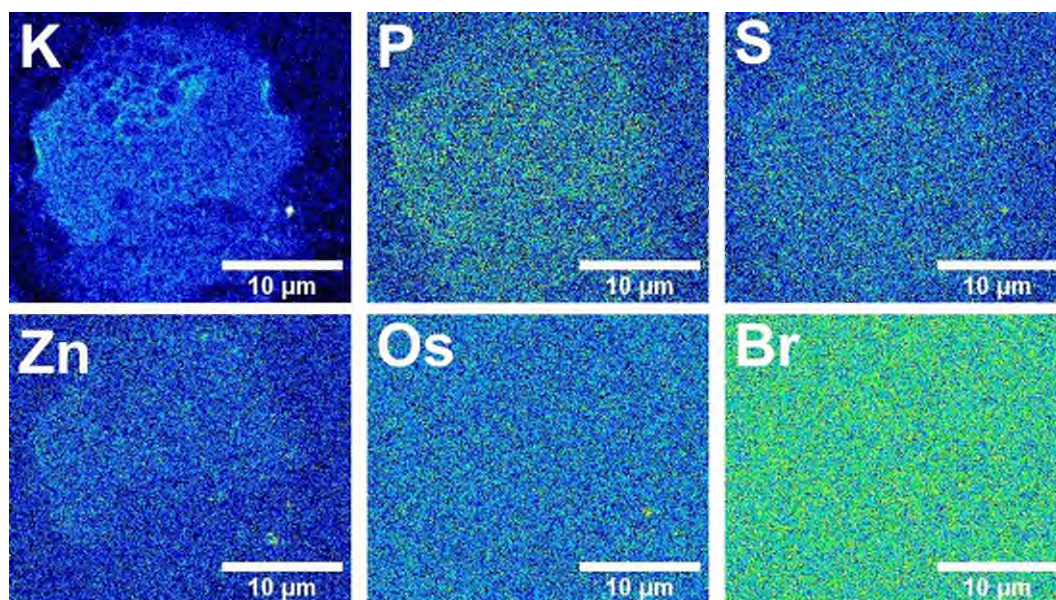


**Figure S25.** Synchrotron-XRF elemental maps of a single cryo-fixed and freeze-dried A2780 (human ovarian) cancer cell (Cell 19, C19) grown on a  $\text{Si}_3\text{N}_4$  membrane obtained using an incident energy of 15 keV: K, P, S, Zn, Os and Br. Maps were collected using 100 nm step size and 0.1 s dwell time. Data were processed in PyMCA toolkit (ESRF),<sup>2</sup> and images were generated in ImageJ for Windows using the 16-colour setting.<sup>3</sup>



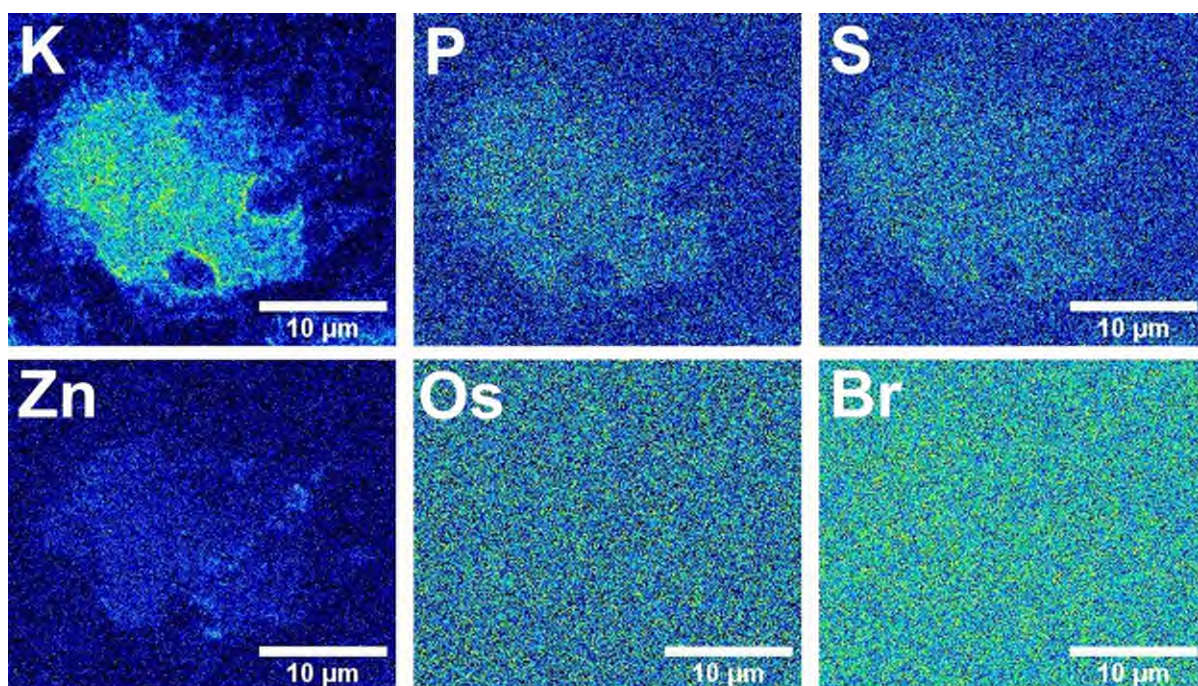


**Figure S26.** Synchrotron-XRF elemental maps of a single cryo-fixed and freeze-dried A2780 (human ovarian) cancer cell (**Cell 20, C20**) grown on a  $\text{Si}_3\text{N}_4$  membrane obtained using an incident energy of 15 keV: K, P, S, Zn, Os and Br. Maps were collected using 100 nm step size and 0.1 s dwell time. Data were processed in PyMCA toolkit (ESRF),<sup>2</sup> and images were generated in ImageJ for Windows using the 16-colour setting.<sup>3</sup>

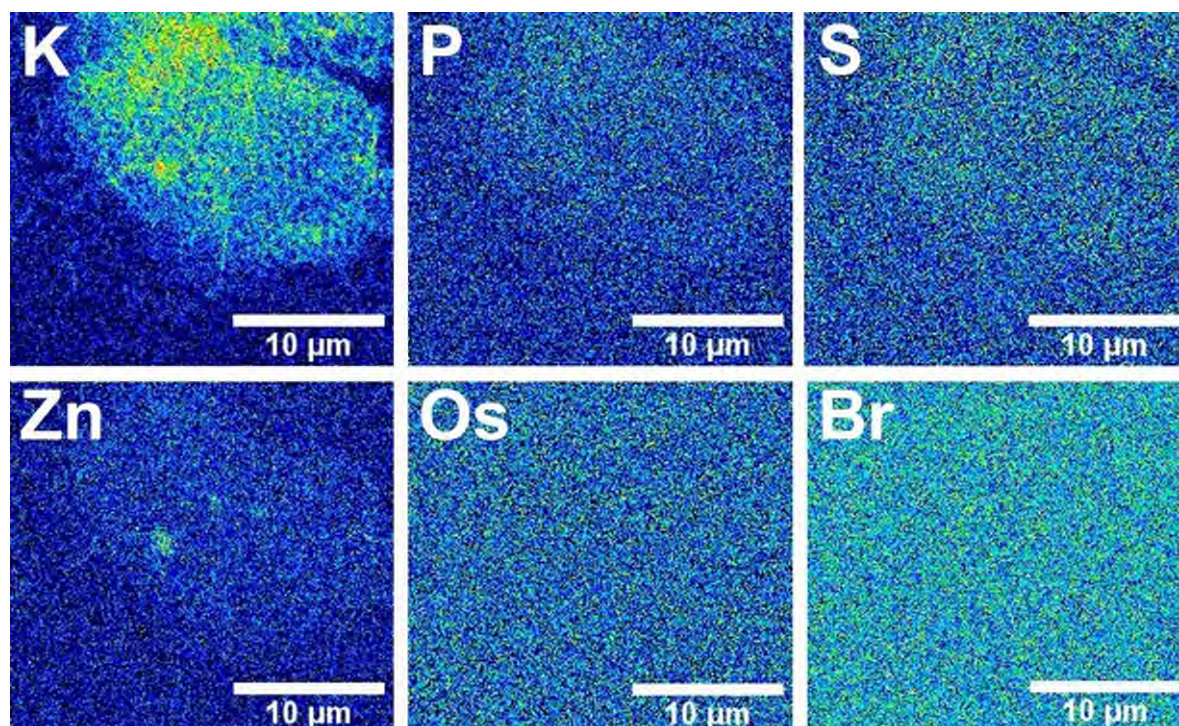


**Figure S27.** Synchrotron-XRF elemental maps of a single cryo-preserved and freeze-dried A2780 (human ovarian) cancer cell (**Cell 21, C21**) grown on a  $\text{Si}_3\text{N}_4$  membrane obtained using an incident energy of 15 keV: K, P, S, Zn, Os and Br. Maps were collected using 100 nm step size and 0.1 s dwell time. Data were processed in PyMCA toolkit (ESRF),<sup>2</sup> and images were generated in ImageJ for Windows using the 16-colour setting.<sup>3</sup>



## XRF maps of A2780 cells treated with 4-PF<sub>6</sub>

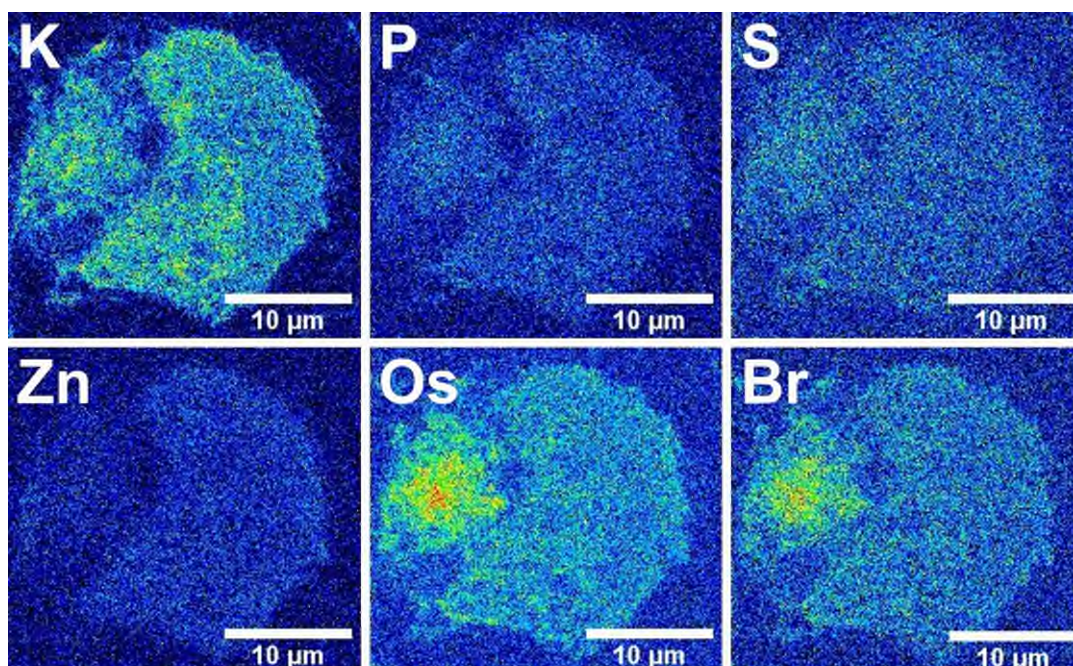


**Figure S28.** Synchrotron-XRF elemental maps of two cryo-fixed and freeze-dried A2780 (human ovarian) cancer cell (**Cell 22, C22**) grown on a Si<sub>3</sub>N<sub>4</sub> membrane and treated with 7× IC<sub>50</sub> (3 μM) **4-PF<sub>6</sub>** for 4 h, obtained using an incident energy of 15 keV: K, P, S, Zn, Os and Br. Maps were collected using 100 nm step size and 0.1 s dwell time. Data were processed in PyMca toolkit (ESRF),<sup>2</sup> and images were generated in ImageJ for Windows using the 16-colour setting.<sup>3</sup>

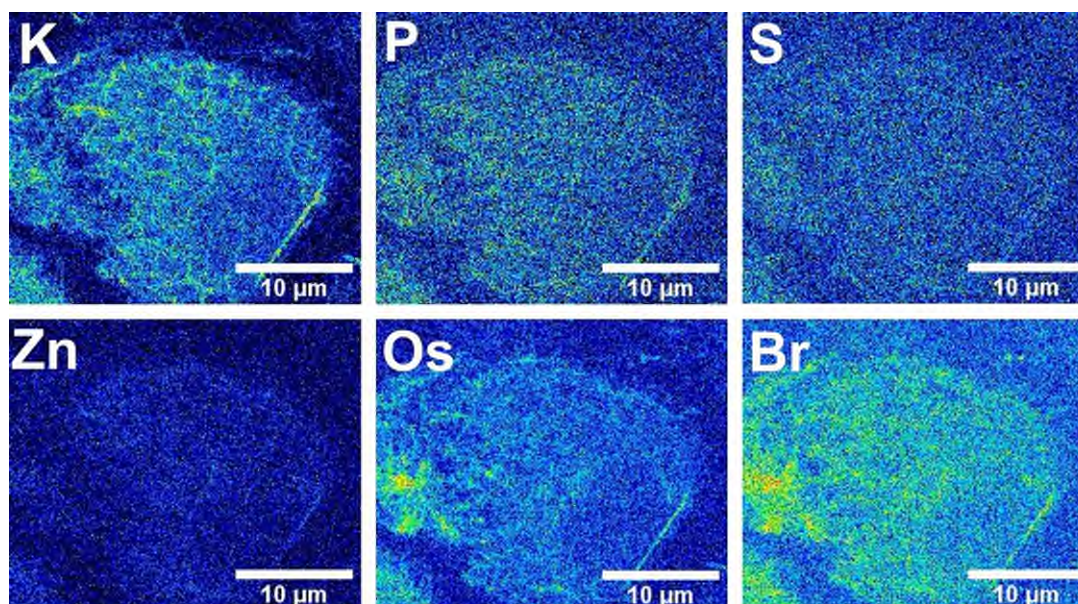


**Figure S29.** Synchrotron-XRF elemental maps of two cryo-fixed and freeze-dried A2780 (human ovarian) cancer cell (**Cell 23, C23**) grown on a Si<sub>3</sub>N<sub>4</sub> membrane and treated with 7× IC<sub>50</sub> (3 μM) **4-PF<sub>6</sub>** for 4 h, obtained using an incident energy of 15 keV: K, P, S, Zn, Os and Br. Maps were collected using 100 nm step size and 0.1 s dwell time. Data were processed in PyMca toolkit (ESRF),<sup>2</sup> and images were generated in ImageJ for Windows using the 16-colour setting.<sup>3</sup>



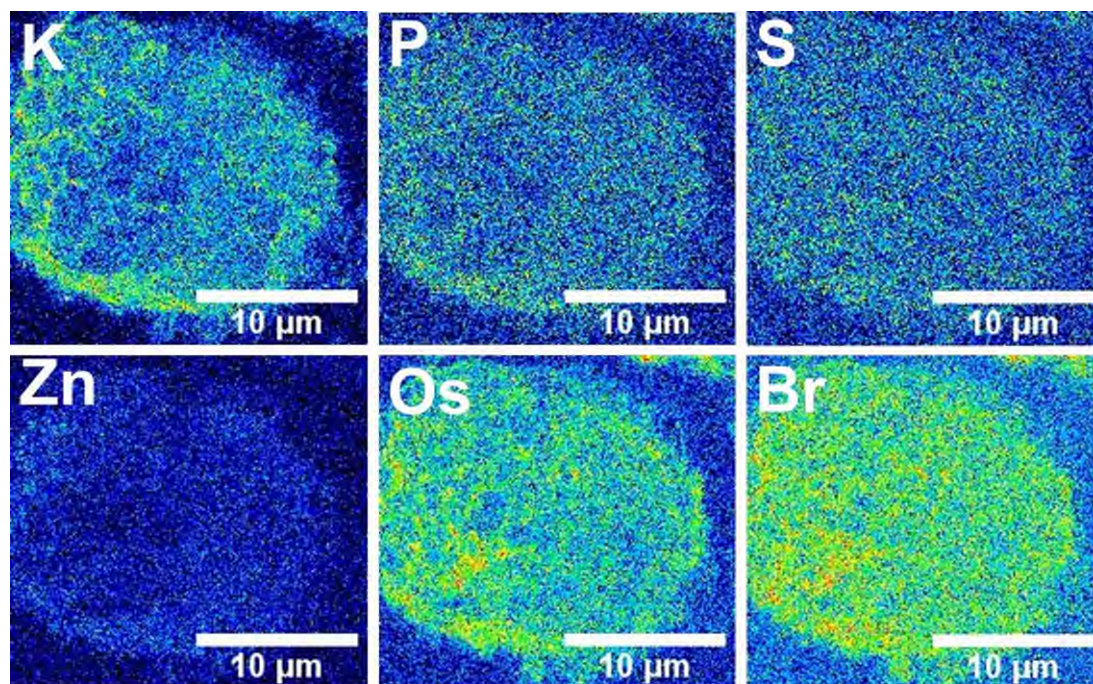


**Figure S30.** Synchrotron-XRF elemental maps of two cryo-fixed and freeze-dried A2780 (human ovarian) cancer cells (**Cell 24, C24**) grown on a  $\text{Si}_3\text{N}_4$  membrane and treated with  $7\times \text{IC}_{50}$  ( $3\ \mu\text{M}$ ) **4-PF<sub>6</sub>** for 4 h, obtained using an incident energy of 15 keV: K, P, S, Zn, Os and Br. Maps were collected using 100 nm step size and 0.1 s dwell time. Data were processed in PyMCA toolkit (ESRF),<sup>2</sup> and images were generated in ImageJ for Windows using the 16-colour setting.<sup>3</sup>

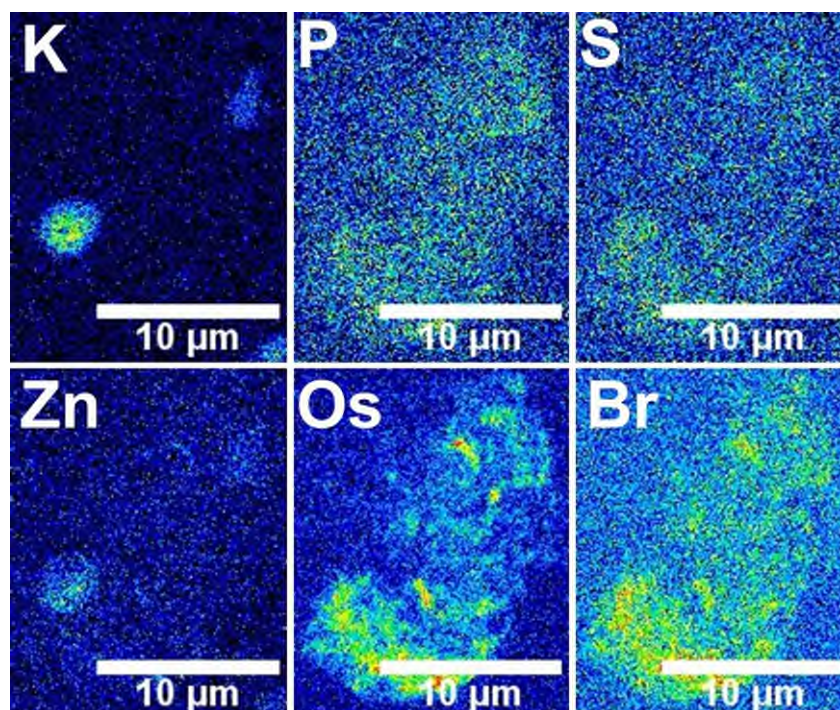


**Figure S31** Synchrotron-XRF elemental maps of two cryo-fixed and freeze-dried A2780 (human ovarian) cancer cells (**Cell 25, C25**) grown on a  $\text{Si}_3\text{N}_4$  membrane and treated with  $7\times \text{IC}_{50}$  ( $3\ \mu\text{M}$ ) **4-PF<sub>6</sub>** for 24 h, obtained using an incident energy of 15 keV: K, P, S, Zn, Os and Br. Maps were collected using 100 nm step size and 0.1 s dwell time. Data were processed in PyMCA toolkit (ESRF),<sup>2</sup> and images were generated in ImageJ for Windows using the 16-colour setting.<sup>3</sup>



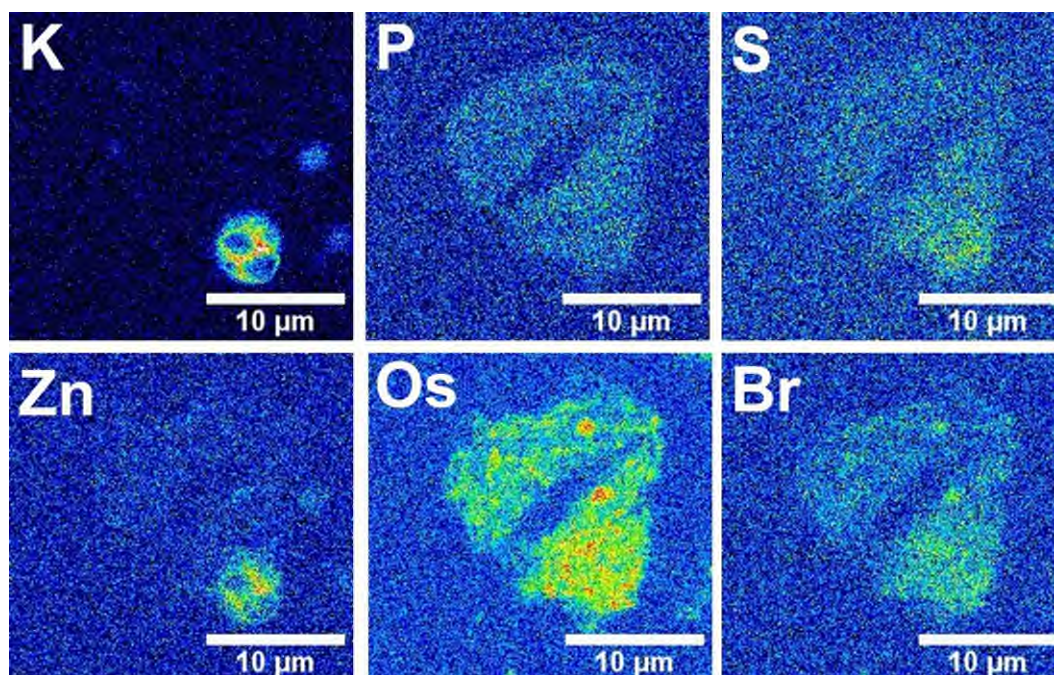


**Figure S32.** Synchrotron-XRF elemental maps of two cryo-fixed and freeze-dried A2780 (human ovarian) cancer cells (**Cell 26, C26**) grown on a  $\text{Si}_3\text{N}_4$  membrane and treated with  $7\times \text{IC}_{50}$  ( $3\ \mu\text{M}$ ) **4-PF<sub>6</sub>** for 24 h, obtained using an incident energy of 15 keV: K, P, S, Zn, Os and Br. Maps were collected using a 100 nm step size and 0.1 s dwell time. Data were processed in PyMCA toolkit (ESRF),<sup>2</sup> and images were generated in ImageJ for Windows using the 16-colour setting.<sup>3</sup>

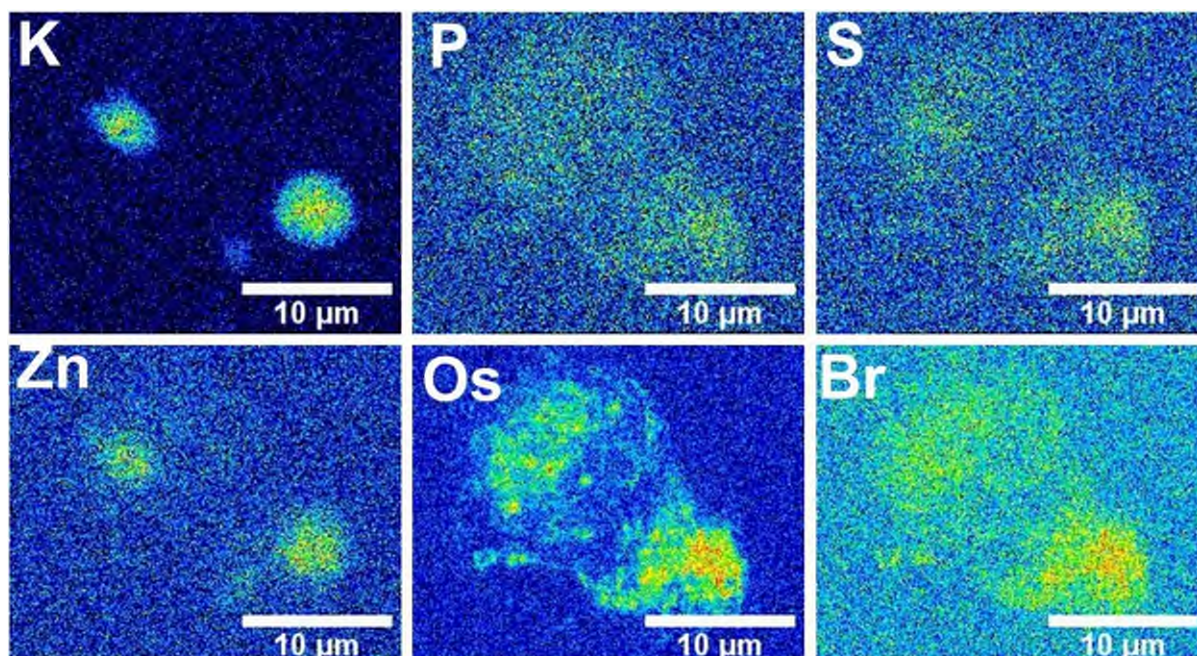


**Figure S33.** Synchrotron-XRF elemental maps of two cryo-preserved and freeze-dried A2780 (human ovarian) cancer cells (**Cell 27, C27**) grown on a  $\text{Si}_3\text{N}_4$  membrane and treated with  $7\times \text{IC}_{50}$  ( $3\ \mu\text{M}$ ) **4-PF<sub>6</sub>** for 24 h, obtained using an incident energy of 15 keV: K, P, S, Zn, Os and Br. Maps were collected using a 100 nm step size and 0.1 s dwell time. Data were processed in PyMCA toolkit (ESRF),<sup>2</sup> and images were generated in ImageJ for Windows using the 16-colour setting.<sup>3</sup>

## Cell areas ( $\mu\text{m}^2$ ) and roundness factors

**Table S6.** Individual and average cell area ( $\mu\text{m}^2$ ) of cryo-fixed and freeze-dried cells as calculated in triplicate using ImageJ software<sup>3</sup>: (i) incubated in complex-free media for 24 h; (ii) treated with  $7\times$  IC<sub>50</sub> of **4-PF<sub>6</sub>** (3  $\mu\text{M}$ ) for 4 or 24 h. No statistically significant differences were observed when using Welch's unpaired t-test, assuming equal variables.

Complex	Cell number	Cell area ( $\mu\text{m}^2$ )	Average cell area ( $\mu\text{m}^2$ )	Roundness Factors	Average Roundness Factor
Untreated	C18	476 $\pm$ 6	371 $\pm$ 71	0.89 $\pm$ 0.02	0.75 $\pm$ 0.16
	C19	383 $\pm$ 12		0.93 $\pm$ 0.03	
	C20	316 $\pm$ 8		0.60 $\pm$ 0.01	
	C21	307 $\pm$ 5		0.59 $\pm$ 0.02	
4-PF <sub>6</sub> (4 h)	C22	487 $\pm$ 5	425 $\pm$ 74	0.94 $\pm$ 0.04	0.84 $\pm$ 0.09
	C23	328 $\pm$ 8		0.75 $\pm$ 0.02	
	C24	461 $\pm$ 1		0.82 $\pm$ 0.02	
4-PF <sub>6</sub> (24 h)	C25	229 $\pm$ 7	188 $\pm$ 40	0.48 $\pm$ 0.01	0.71 $\pm$ 0.22
	C26	197 $\pm$ 1		0.98 $\pm$ 0.01	
	C27	138 $\pm$ 5		0.66 $\pm$ 0.02	

## Elemental colocalization statistics

**Table S7.** Elemental co-localisation statistics (R-value and Spearman Rank Correlation) between osmium and bromine in cryo-preserved and dehydrated A2780 ovarian cancer cells grown on silicon nitride membranes and treated with  $7\times$  IC<sub>50</sub> of **4-PF<sub>6</sub>** (3  $\mu\text{M}$ ) for 4 or 24 h (no recovery) as determined in Image J.<sup>3</sup>

Time / h		R-value	Mean R-value	Spearman Rank Coefficient	Average Spearman Rank Correlations
4	C22	0.32	0.33 $\pm$ 0.04	0.28	0.30 $\pm$ 0.06
	C23	0.29		0.26	
	C24	0.37		0.37	
24	C25	0.46	0.38 $\pm$ 0.08	0.38	0.30 $\pm$ 0.06
	C26	0.31		0.25	
	C27	0.37		0.28	

## ES10 References

1. J. Tönnemann, J. Risse, Z. Grote, R. Scopelliti and K. Severin, Efficient and Rapid Synthesis of Chlorido-Bridged Half-Sandwich Complexes of Ruthenium, Rhodium, and Iridium by Microwave Heating, *Eur. J. Inorg. Chem.*, 2013, **2013**, 4558-4562.
2. V. A. Solé, E. Papillon, M. Cotte, P. Walter and J. Susini, A multiplatform code for the analysis of energy-dispersive X-ray fluorescence spectra, *Spectrochim. Acta B.*, 2007, **62**, 63-68.
3. C. T. Rueden, J. Schindelin, M. C. Hiner, B. E. DeZonia, A. E. Walter, E. T. Arena and K. W. Eliceiri, ImageJ2: ImageJ for the next generation of scientific image data, *BMC Bioinform.*, 2017, **18**, 529-529.
4. Y. Fu, A. Habtemariam, A. M. Pizarro, S. H. van Rijt, D. J. Healey, P. A. Cooper, S. D. Shnyder, G. J. Clarkson and P. J. Sadler, Organometallic Osmium Arene Complexes with Potent Cancer Cell Cytotoxicity, *J. Med. Chem.*, 2010, **53**, 8192-8196.